Steady-State Two-Phase Flow Conductance in a 2D Micromodel

E. J. M. (Ewald) Obbens

Thesis supervisors: Prof. W. R. Rossen & Prof. J. Bruining

Delft, Netherlands, August 31st 2020

Delft University of Technology

Preface

This thesis continues on the work of J. Holstvoogd (2020) and G. Hadjisotiriou (2020). The goal of this series is to investigate the viability of steady-state two-phase flow in a 2D micromodel. Their work focusses mainly on the network aspect of the flow, whereas this thesis looks at the pore-scale flow processes. By combining the results of Hadjisotiriou (2020) with those of this thesis, it has been possible to create an estimate for the relative amount of liquid and gas to flow through a 2D network.

I would like to thank Prof. W. R. Rossen and Prof. J. Bruining for giving encouragement, enthusiasm and invaluable assistance to me. Another thank you is in order for B. Artola for answering my questions concerning COMSOL™ and to G. Hadjisotiriou for answering my questions concerning his work.

Ewald Obbens
Delft
August 31st 2020

Summary

This study is part of a larger effort to evaluate the use of microfluidics to represent foam generation and flow in geological porous media (Rossen, 2008). Specifically whether it is possible to have flow in a microfluidic device without fluctuating occupancy of pores and pore throats. Although there is no foam created during the study, three of the main foam generation mechanisms are discussed. The 2D network consists of a 32x32 square lattice of cylindrical pillars, where all the pillars are surrounded by at the top and bottom by a liquid film that constricts the gas flow. The pores and pore throats are filled with gas or water. The gas flow paths are gas filled pores connected with gas filled pore throats. The water flow paths are pillars connected with water filled pores or pore throats. Liquid/gas bridges are necessary for the two phases to flow simultaneously through the network. An equivalent conductance for the gas networks is obtained by Hadjisotiriou (2020). But for that value to have any relation with that of the water network, the gas and water flow should be simulated within shapes that fit into one another under the same conditions. Because the paths in the network could have countless different variations, these paths are broken up into the smallest repeated segments. Then the total resistance of a path is obtained from a combination of these segments. Two unique segments are identified for the gas paths and four for the water paths. The segments are created in COMSOL™. A conductance value is obtained for each segment. With these values it is possible to calculate the total conductance for both the gas and water networks. The result is a fraction of water flow relative to gas flow of around 0.015. This means that only a small amount of water flow can be sustained by the network without fluctuating the occupancy of pores and pore throats. This makes it hard to explore foam generation in a microfluid device. It also means that two-phase flow in a microfluidic device is not representative of that in 3D geological porous media, except for in some exceptional circumstances.

Table of Contents

1. Introduction

Two-dimensional microfluidic networks are used to obtain knowledge about the flow through porous media. However, as these networks are two-dimensional and simplified, they might not be able to fully represent the processes that come into play in three-dimensional geological porous media. But conclusions drawn from the two-dimensional networks could be the basis for a better understanding of the behaviour in three dimensions. This thesis continues on the work of Holstvoogd (2020) and of Hadjisotiriou (2020). The goal is to figure out whether it is possible to have stable simultaneous two-phase gas-water flow in a microfluidic network. Stability here means that the flow paths do not change with time. This is known to be possible in 3D pore networks of geological porous media. The microfluidic networks are occupied by the gas and water phases so that the ratio of the conductivities or resistivities can be determined between the gas and water phases. The flow paths for both phases can be split up into smaller repeating elements. In the work of Hadjisotiriou (2020) the networks are created and total counts for each of the unique elements per flow path are obtained. The possibility of the stable flow is not certain in a two-dimensional network, as percolation theory shows that only one phase could flow through a 2D isotropic media at the same time. However, it could be possible with the occurrence of liquid bridges in the network where the water and gas cross in the same pore throat. The flow rates through those elements are calculated using the Microfluidics software module of COMSOL Multiphysics.

1.1 Foam generation mechanisms

This study is part of a larger effort to evaluate the use of microfluidics to represent foam generation and flow in geological porous media (Rossen, 2008). Specifically, the issue is whether flow in a microfluidic device is possible without fluctuating occupancy of pores and pore throats. Water is the strongly wetting phase, and surfactant occupies the liquid-gas interfaces (Rossen, 1996). Because the larger goal is to evaluate the use of microfluidics to represent the creation of foam, there is no foam in the network in this study: only gas and water, with surfactant dissolved in the water and on the interfaces. Foam is defined in Rossen (1996) as 'a dispersion of gas in a liquid such that the liquid phase is interconnected and at least some gas flow paths are blocked by lamellae'. Foams are modelled as a multiphase problem where gas-filled pores have their walls lined with water. The three main mechanisms for foam generation are shown in *figure 1*.

Snap-off

Snap-off happens when enough water accumulates between two grains to connect them with water and block the flow of gas (Rossen, 1996; Kovscek et al., 2007). This process thus involves fluctuating occupancy of the pore throat.

Lamella division

Lamella division happens when one lamella is pushed into a pore body with multiple pore throats. This could either break up the lamella or split it up into multiple lamellae that continue moving through those pore throats.

Leave behind

Water gets displaced when gas is first injected into the porous medium. If the gas moves through two side by side pores, a water lamella will be left behind between the grains parallel to the gas flow direction.

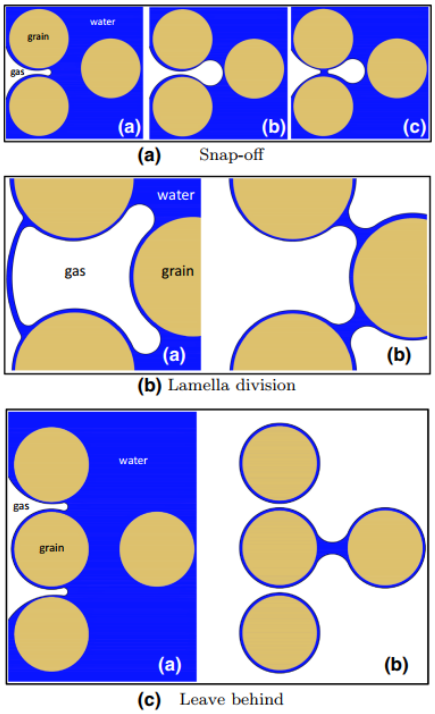

Figure 1: The three foam generation mechanisms from (Almajid & Kovscek, 2019)

1.2. Microfluidic networks

If the network we consider were to be created experimentally it would start shaped like a two-dimensional square lattice where the nodes are cylindrical pillars. *Fig. 2* shows a schematic of the microfluidic device as a whole, on the large scale. Figures below illustrate the network structure on the small scale The pillars located in this network are of a size in the range of tens of microns.

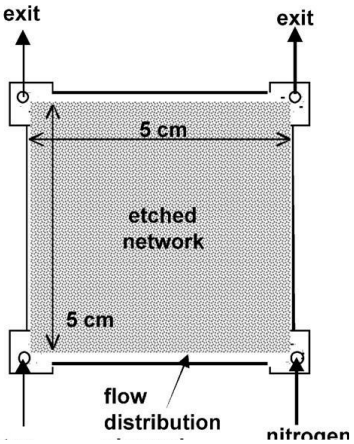

Figure 2: experimental version of the micromodel from (Kovscek et al., 2007)

Initially, the network would be filled with water, after which gas will be injected into the grid to displace most of the water. But not all the water will be removed from the lattice; some water stays behind in pore bodies and pore throats. In addition, even in pores filled with gas, water, as the strongly wetting phase, surrounds the pillars and can form connections between the pillars, described below. The connections of the water from pillar to pillar forms an essential part of the network the water will flow through. The gas-filled pores connected through gas-filled pore throats form the network the gas flows through.

One concern is that these 2D flow experiments might not be able to recreate the same foam generation processes that happen in a three-dimensional porous medium. One of these differences is that it is hard to maintain two-phase flow in a steady state in a two-dimensional network as the liquid and gas flow paths have to compete for the pore occupancy to continue flowing. In

three-dimensional networks, this is different because the paths could pass around one another in the third dimension.

1.3. The two-dimensional model

A percolation model in the shape of a lattice is used to represent the micromodel. In this lattice, disorder is introduced using bond percolation resulting in a lattice consisting of a grid of cylindrical shaped grains where the pores and throats are either filled with gas or water. The gas connectivity is established by assigning a random value to every bond. If the bond has a value above the percolation threshold it will allow gas to flow and have a conductivity with a value of 1, if it has a lower value it will block gas and have a conductivity value of 0. (Hunt & Sahimi, 2017). When a pore or throat adjacent to a pillar is filled with gas, the pillar has liquid in its corners that restricts the gas flow. This is shown in *Fig. 3*.

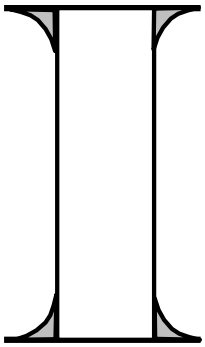

Figure 3: Schematic showing the side-view of a pillar with water in its corners. (Rossen, 2020)

To obtain the steady-state two-phase flow in a two-dimensional micromodel, the gas and water flow paths have to be able to cross each other. This would be possible with the establishment of liquid bridges which allow water and gas to cross through the same pore throat. These liquid bridges would have to be stable so that the liquid stays in place and snap-off does not occur.

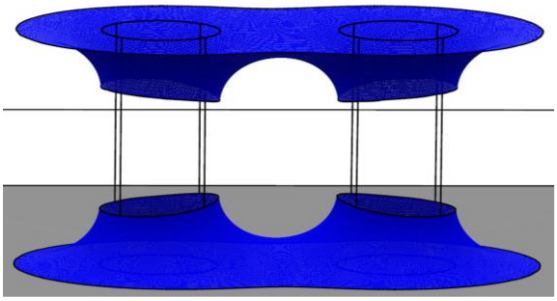

Figure 4: An example of a liquid bridge. The pillars are the vertical cylinders. The location of the water is shown in blue. The gas flows in or out of the page through the gap.(Cox, 2020)

The gas networks created in the work of Hadjisotiriou (2020) are represented in two ways, one contains only the gas backbone plotted as a network graph in MATLAB, with the shortest gas path highlighted in green. This representation can be seen in *Fig. 5*.

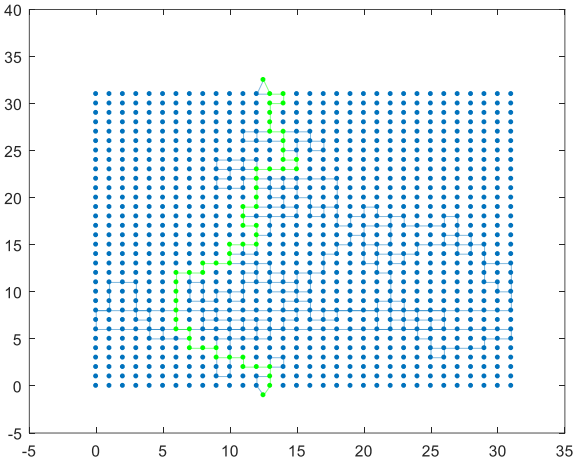

Figure 5: Gas network representation. The nodes are the gas filled pores and the edges the gas filled pore throats. (Hadjisotiriou 2020)

The other representation is created in Excel. A sample of this is shown in *Fig. 6*. In this representation of the network, both the gas and water are shown. The pillars are the dark grey squares, and although they are shown as square-shaped, the plan view of them in the model will be circular as they are cylindrical. The green blocks are the gas-filled pores and pore throats that are connected to the gas backbone that flows from one side to another and top to bottom. The black

squares are the gas-filled pores and pore throats that are dead ends connected to the backbone. The blue squares are showing the pores and pore throats that form the shortest or simplest paths that the water can use to flow across the network. The light grey squares show the water-filled pores and pore throats. The squares with a green centre and blue border show where the liquid bridges would be to allow water flow across these paths.

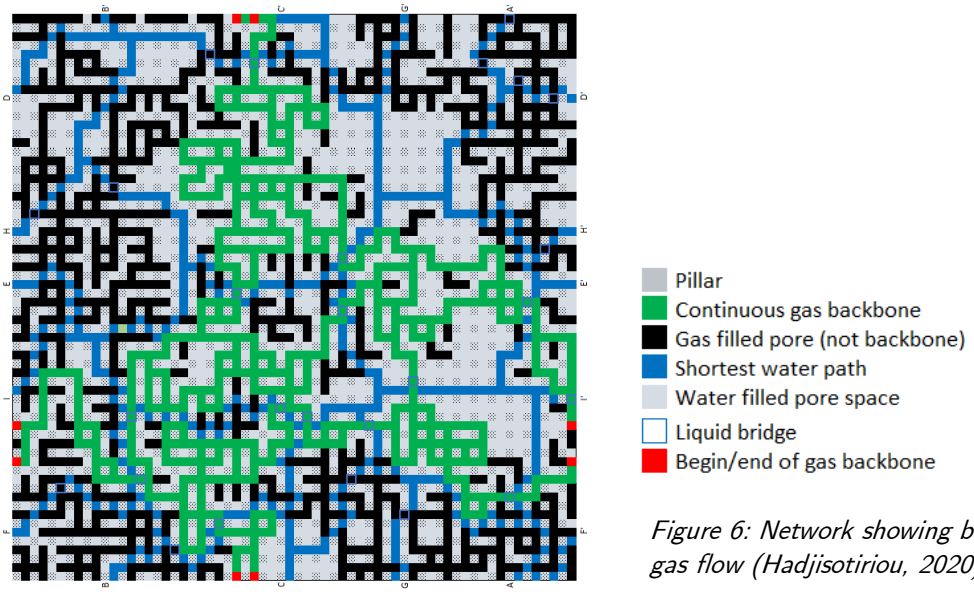

Figure 6: Network showing both the water and gas flow (Hadjisotiriou, 2020)

2. Conductivity on a pore-scale

2.1. Gas conductivity

In Hadjisotiriou (2020) the same methods used to determine the equivalent electrical resistance in a network are used to solve for the network-wide gas resistance. That calculation is based on an estimate of the resistance of gas flow through the individual segments of the network.

A conductance/resistance value for the gas network can now be established. But for that value to have any relation with that of the water network, the gas and water flow should be simulated within shapes that fit into one another under the same conditions. Because the paths in the network could have countless different variations, these paths are broken up into the smallest repeated segments. So that the total resistance of a path is obtained from a combination of these segments.

The gas path can be split up into two different segments. The first is named Rg and represents the gas flow from one pore through a pore throat into another pore. The other is named Rgb and represents the gas flow from a pore through the gap in a liquid bridge into another pore.

Rg, gas flow through pore throat.

Fig. 7 shows an example of an Rg as represented in one of the networks of Hadjisotiriou (2020). It shows how the domain starts in the middle of one pore body and ends to the middle of the next pore body. This example shows the gas path being straight before and after the interval. We use this to simulate the flow through any gas occupied pore throat in the network, even if the gas has to change direction before or after the interval. This is done under the assumption that because the gas is so much less viscous than the liquid that there is no significant difference for the gas in going straight or going through a corner in a wide pore body. The pressure contour plots in the Appendix show that by far most of the pressure drop is in the constriction, not in the pore body.

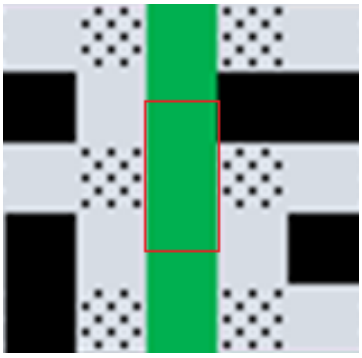

Figure 7: An example of Rg is encircled in red.

Fig. 8 shows the geometry as it has been made in COMSOL™. The gas flows within the walls of this geometry. The square plane with its normal vector pointing along the negative x-direction is where the gas flows into the segment. It then flows through the narrow part which represents a pore throat, to then flow out from the square on the opposite side. The reason that the pillars shape around the pore throat is curved instead of straight, as one would expect from the flow through two pillars, is because there is a liquid film stuck on every pillar, illustrated in *Fig. 3*.

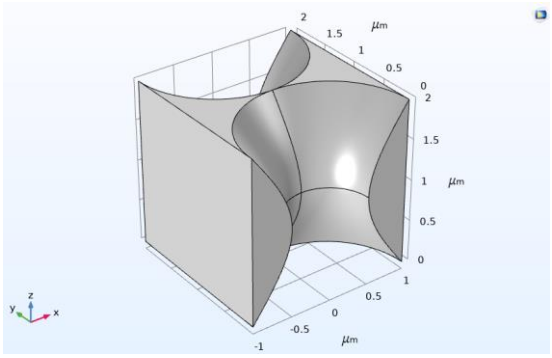

Figure 8: The geometry of the Rg shape, which represents the gas flow through one pore throat, rom one pore body to another. Note that the pillars on either side of the throat are assumed to have liquid films at the top and bottom of the pillar, restricting gas flow.

Rgb, gas flow through a liquid bridge.

Fig. 9 shows an example of the gas flow through a liquid bridge as represented in one of the networks. It shows how the domain starts in the middle of one pore body and ends in the middle of the next pore body. In this case, the example shows that the interval begins and ends in the middle of a corner. The reason that the geometries still fit together is explained in the previous subchapter.

Figure 9: An example of Rgb is encircled in red.

Fig. 10 shows the geometry as we created it in COMSOL™. The gas flows within the walls of this geometry. The channel for gas flow is much more restricted than in *Fig. 8* above. Our collaborators at the University of Aberystwyth have shown that the bridge can be sustained to much lower capillary pressure than that shown in *Fig. 4* above; hence we use a narrower geometry for gas to flow. The square plane with its normal vector pointing along the negative x-direction is where the gas flows into the shape. It then flows through the narrow part which represents a pore throat, to then flow out from the square on the opposite side. The middle part is noticeably narrower compared to the Rg shape because of the constriction caused by the liquid bridge.

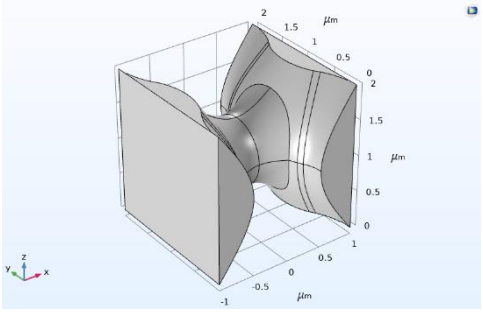

Figure 10: The geometry of the Rgb shape, which represents the gas flow through one pore throat. From the centre one pore body to another. Note that the liquid is shown to bridge between the pillars on opposite sides of the throat, restricting gas flow.

2.2. Liquid conductivity

To obtain the flow rate ratio between the gas and water backbone, First, the liquid flow paths are identified. Then count the number of segments of different types, listed below, in each path. For each segment, an example is shown below of where to find it inside of a network. The flow of the liquid will pass through these segments. Calculate resistance to flow in that path (sum of the resistance of all segments), assuming the path is independent of and parallel to all others. If paths are in parallel, total conductivity to liquid is the sum of conductivities of all those paths. Leaving out some paths may underestimate conductivity. Leaving out resistance to flow in liquid-filled pores and throats, and assuming all paths are in parallel (when they share some segments) could over-estimate conductivity. Flow enters through the vertical surface on the left and exits through the one on the right. The vertical surface corresponds to the middle of a pore throat in the case of the water geometries. The pressure and velocity results showing what the flow through the geometries looks like can be found in the Appendix.

R1, Waterflow around a corner

Fig. 11 shows a schematic of how water flows across a pillar to either the left or right. By doing this, it flows around a gas-occupied pore body.

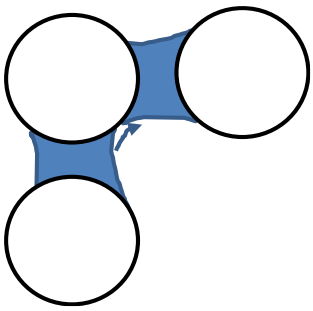

Figure 11: Schematic of three pillars connected by water to form a corner shape. (Holstvoogd, 2020)

Fig. 12 shows an example of the water flow through a corner as represented in one of the networks of Hadjisotiriou (2020). It shows how the domain starts in the middle of one pore throat and ends in the middle of the next pore throat.

Fig. 13 shows the geometry as it has been created in COMSOL™. The water flows within the walls of this geometry. The plane with its normal vector pointing along the negative x-direction is where the liquid flows into the shape. It then flows around a pillar, to flow out from the plane with its normal vector pointing along the negative y-direction.

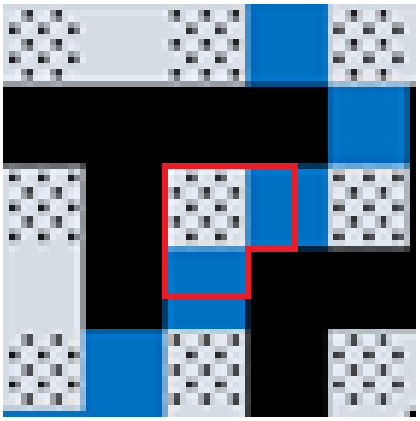

Figure 12: An example of R1 is encircled in red. Water must pass along the top and bottom edges of a pillar to get around a gas-occupied pore body (in black).

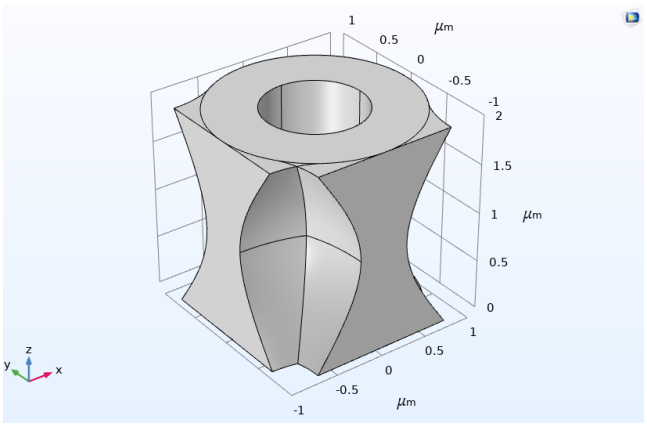

Figure 13: The geometry of the R1 shape which represents one corner in the water flow path. The flow enters in the middle of a pore throat and exits in the middle of a pore throat perpendicular to the initial direction.

R2, Water flow going straight across a pillar

Fig. 14 shows a schematic of how water flows straight past a pillar.

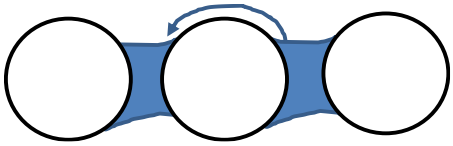

Figure 14: Schematic of three pillars connected by water with the water flowing straight across the middle pillar. (Holstvoogd, 2020)

Fig. 15 shows an example of the water flow through a corner as represented in one of the networks. It shows how the domain starts in the middle of one pore throat and ends in the middle of the next pore throat on the other side of the pillar.

Fig. 16 shows the geometry as it has been made in COMSOL™. The water flows within the walls of this geometry. The plane with its normal vector pointing along the negative x-direction is where the gas flows into the shape. It then flows around a pillar, to the flow out from the plane with its normal vector pointing along the positive x-direction.

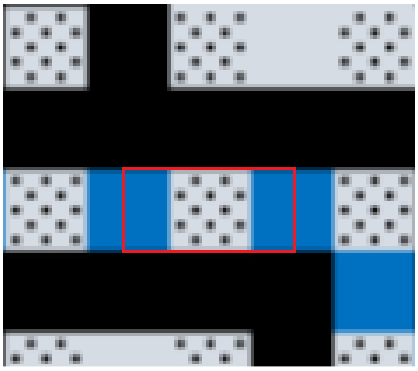

Figure 15: An example of R2 is encircled in red. Water must pass along the top and bottom edges of a pillar to get from one liquid-filled throat to another, with gas-filled pore bodies on either side).

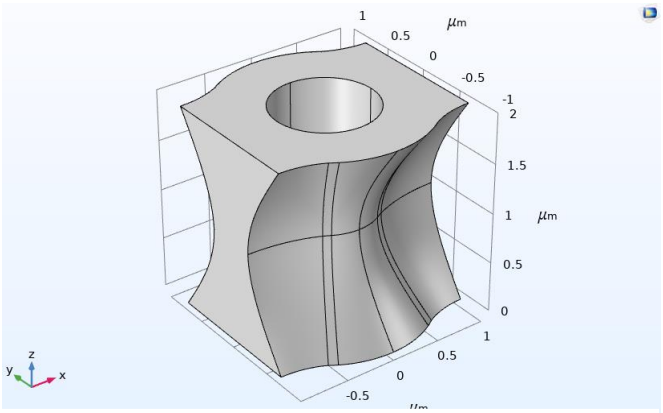

Figure 16: The geometry of the R2 shape which represents one straight part in the water flow path. The flow enters in the middle of a pore throat and exits in the middle of a pore throat opposite of it past the pillar.

Rb, liquid bridge

Rb is the shape representing the liquid bridges. The bridge itself is located in between two pillars. For the segment to connect to the others, the flow has to go from one pore throat past two pillars before it reaches the other pore throat. This causes there to be four variations of this shape. The difference arises from which direction the water flows in or out of the geometry.

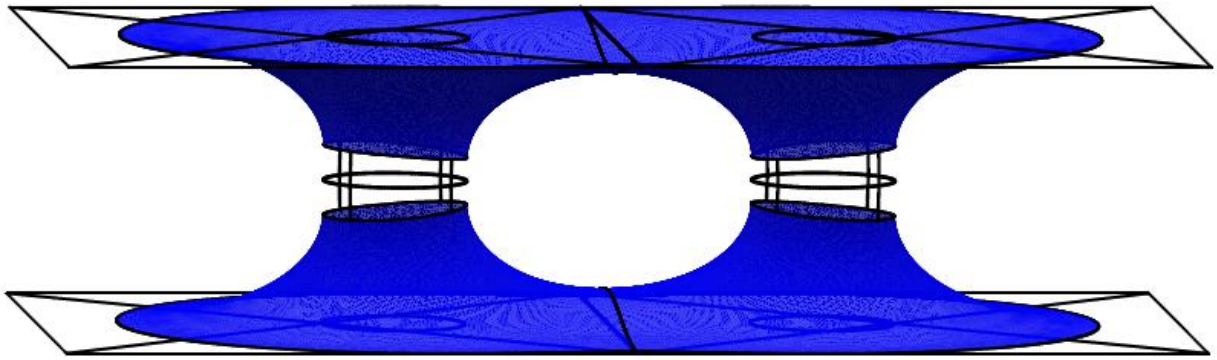

Figure 17: The model the geometry for the liquid bridge is based on. (Cox, 2020)

Rb1, liquid bridge shape with straight flow past the two pillars.

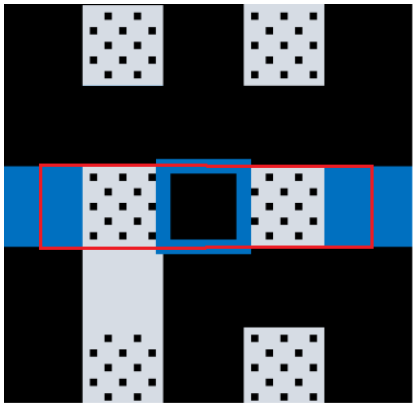

Figure 18: An example of Rb1 is encircled in red. Water films at the top and bottom of two pillars must connect across a gas-filled pore throat. The liquid-filled throats are on opposite sides of the pillars.

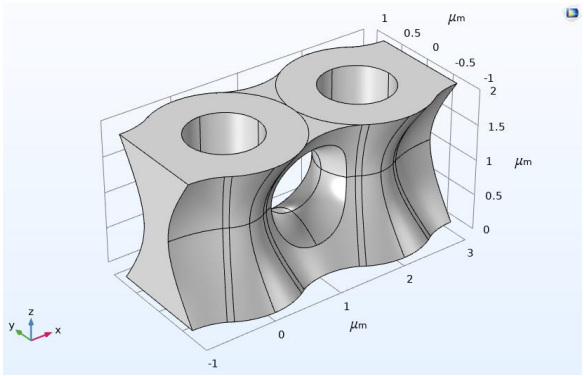

Figure 19: The geometry of the Rb1 shape, which represents a liquid bridge with straight flow past the two pillars. The flow enters in the middle of a pore throat before the first pillar and exits in the middle of a pore throat opposite from it past the second pillar.

Rb2, liquid bridge shape with straight and corner flow past the two pillars.

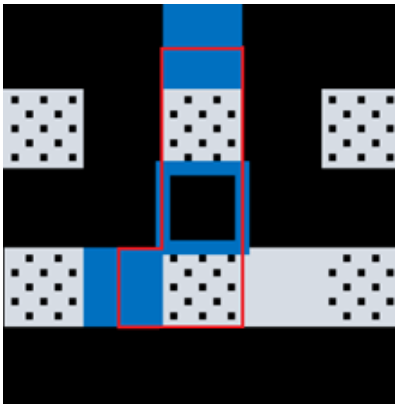

Figure 20: An example of Rb2 is encircled in red. Water films at the top and bottom of two pillars must connect across a gas-filled pore throat. The liquid-filled throats are on located on different sides of the opposing pillars.

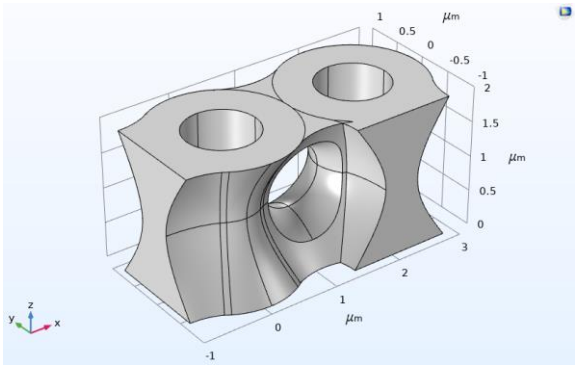

Figure 21: The geometry of the Rb2 shape, which represents a liquid bridge with straight flow past one pillar and a corner around the second pillar. The flow enters in the middle of a pore throat before the first pillar and exits in the middle of a pore throat perpendicular from it past the second pillar.

Rb3, liquid bridge shapes with flow through two corners.

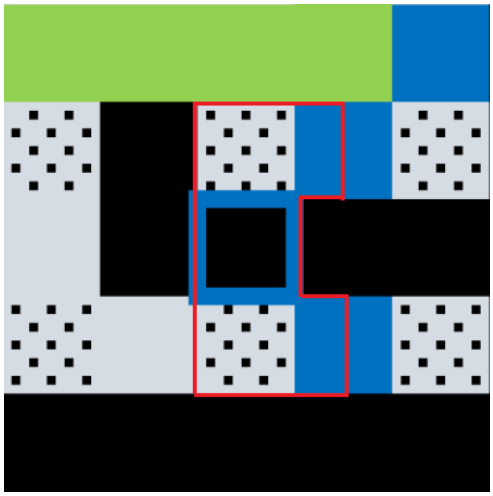

Figure 22: The geometry of the Rb3 shape which represents a liquid bridge with corner flow past both pillars. The flow enters in the middle of a pore throat before the first pillar and exits in the middle of a pore throat in line from it past the second pillar.

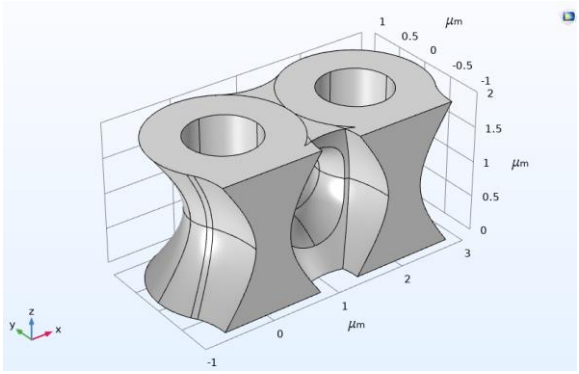

Figure 23: An example of Rb3 is encircled in red. Water films at the top and bottom of two pillars must connect across a gas-filled pore throat. The liquid-filled throats are on located on the same side of the opposing pillars.

Rb4, liquid bridge shape with flow through two opposite corners.

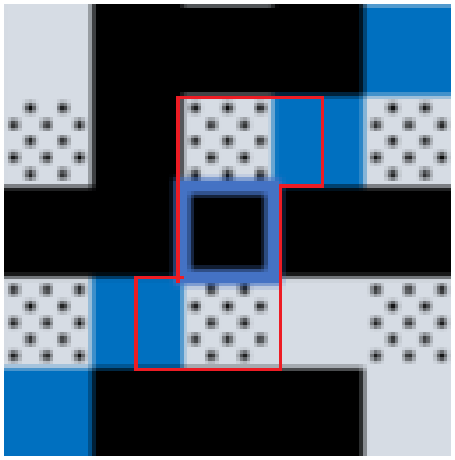

Figure 24: An example of Rb4 is encircled in red. Water films at the top and bottom of two pillars must connect across a gas-filled pore throat. The liquid-filled throats are on located on the different sides of the opposing pillars.

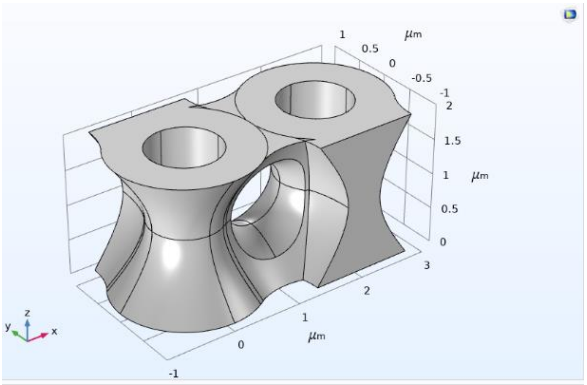

Figure 25: The geometry of the Rb4 shape which represents a liquid bridge shape with corner flow past both pillars. The flow enters in the middle of a pore throat before the first pillar and exits in the middle of a pore throat parallel but not in line to it.

3. The Microfluidics/Creeping flow module in COMSOL

The flows at micron scales are at a scale much smaller than those of macroscopic flows. The main advantage of doing experiments on these microfluidic structures is that it is possible to see directly what is happening within the medium. This is also approximately the scale of flow in geological pore networks.

When the size of the fluid flow is decreased, the properties related to the surface forces in the system become more important than the ones that scale with the fluid volume. The Reynolds number (Re) is the ratio between the viscous and the inertial forces. It is generally very low for microfluidic systems, causing the flow to be laminar.

For all the models the creeping flow module in COMSOL is chosen, as it includes all the functionalities needed for the flow at this scale. It is used for the simulation of single-phase fluid flows at low Reynolds numbers, where the inertial term can be neglected in the Navier-Stokes equations. Even though it is used to compute single-phase fluid flows, it is possible to use it for our simulations. This is because the water and gas interfaces do not change during steady-state flow; the shape of the geometry stays the same, which makes it possible to look at the flow of one phase at a time.

The default boundary condition for both fluids on the walls of the network is No Slip. This means that the fluid velocity is zero relative to the wall velocity. This boundary condition is used where either fluid has an interface with a solid, so when it would touch a pillar or top or bottom of the plate. As noted above, the water contains dissolved surfactant and would have surfactant on its

interface with the gas. In some cases, this acts as a rigid layer, also with a no-slip boundary condition (Ransohoff and Radke, 1988; Rossen, 2003). In other cases the interface is fluid, and a zero-shear-stress boundary condition would apply to the liquid here. The gas is less viscous than liquid; it has no-slip boundary conditions on both solid boundaries and its interfaces with liquid.

We choose the model assumptions to be favourable towards the water flow rate so that in the end the estimate of water flow that can be sustained is a generous over-estimate. Therefore we assume that the water/gas interface imposes a zero-shear-stress boundary condition for the liquid. This will allow the water to flow freely on those boundaries, increasing the total flow rate.

Because there is a net flow in and out of the domain, both an inlet and outlet are set with a pressure difference of 1 Pascal for every calculation of conductivity.

4. Results

In Hadjisotiriou (2020) the gas flow through the pore throats (segment Rg) was given a resistance value of 1 unit each. As a result, the equivalent resistance of the whole network could be expressed by a certain number of Rg segment resistances. If the resistance value for Rg is 1, then relative to this the resistance values for all the other segment geometries can be obtained. Then it is be possible to express the water/gas flow ratio of the network as a ratio of the resistance of the water and gas networks.

The flow rate (Q) through every segment for different materials and boundary conditions (assuming a pressure difference of 1 Pa across the segment) can be found in Appendix B1. To obtain the relative resistance value for all the flow segments it is necessary to take the multiplicative inverse of the flow rate first (1/Q). This is because conductance and resistance have an inverse relationship. To then normalize this value to 1 for the Rg geometry, all the 1/Q values have to be divided by the 1/Q value for segment Rg.

With these normalized resistance values for all the liquid flow geometries, the total resistance values for all the water flow paths can be calculated. In appendix B3 all the networks from Hadjisotiriou (2020) are shown. In the tables, it shows the counts for R1, R2 and Rb segments per flow path. The liquid segment counts of Hadjisotiriou had to be adjusted as follows. The domain of one Rb as defined here overlaps with two of either R1 or R2 as counted by Hadjisotiriou because he neglected the geometry of the path near the bridge (the focus of *Figs. 18-25* above). To solve this overlap of the segments, the Rb geometry domain has been extended to include two pillars and start and end in the middle of the pore throat before them, as discussed above. This allows the Rb segment to connect seamlessly with the R1 and R2 segment. But that also means that there are still two segments for either R1 or R2 that would overlap with the Rb. To solve this, two counts of R2 (as counted by Hadjisotiriou) for every Rb have been subtracted from the total counts for every flow path. R2 is chosen as it has the higher resistance value of the two, and removing them would benefit the water flow more. Another issue with the count of Rb is that there is no distinction for the four different variations it can occur in. To solve this without having to recount the shapes, the resistance value for Rb3 has been used as it is the lowest of the four. So it is as beneficial towards the water flow as possible.

The resistance values are determined for the three different shapes in the water flow paths. So now by multiplying these values with the total counts and summing up these values, the total resistance per liquid flow path is determined. The flow paths are divided up into those connecting horizontally or vertically across the grid. To obtain the equivalent resistance for either one of the directions, the formula for parallel resistances in a circuit is used. This results in an equivalent resistance that is lower than the resistance for any individual flow path.

Three different viscosities have been used in the gas geometries to calculate the flow rates for H_2O, CO_2 and N_2. The reason that H_2O is being used, even though it is a liquid, is because using the same material makes it possible to compare the resistances (in effect, relative permeability, excluding viscosity) between the liquid and gas geometries. The CO_2 and N_2 viscosities are used to show how the relative mobility scales with the fraction of the viscosities between the liquid and the gas.

All simulations are done at a temperature of T = 293.15 K and Pressure = 1 atm.

With these settings, the viscosity values are as in *Table 1*.

Table 1: The viscosity values of the materials.

Material	Viscosity μ [Pa·s]
H_2O	0.00100935
N_2	0.000017436
CO_2	0.0000146885

In *Table 2* a summary of the results for the gas and water networks using slip conditions using the same viscosity for the flow.

Because the calculated values for the resistances use the same viscosity throughout the networks, the values for the water networks have to be multiplied by a viscosity factor. The viscosity factor is the ratio of the liquid and gas viscosities. For nitrogen, the factor used is about 50.

The following calculation is done with the average values from table 2 to calculate the water/gas flowing fraction:

$$\frac{C_{h\&v}}{C_{gas} * \left(\frac{\mu_{liquid}}{\mu_{gas}}\right)} = \frac{0.02855}{0.037 * 50} \approx 0.015$$

Table 2: Summary of the results when the same viscosity material is used through the gas and water network under slip conditions. C gas is the total conductance of the gas flow. C horizontal is the total conductance of the water network that flows horizontally. C Vertical is the total conductance of the water network that flows vertically. R h & v is the equivalent conductance if the water can flow through both the horizontal and vertical network at the same time.

Network	C gas	C horizontal	C vertical	C h & v
1	0.0303	0.016759	0.010098	0.026856
2	0.0341	0.01111	N/A	0.01111
3	0.0375	0.017581	0.039647	0.057228
4	0.0372	0.014084	0.016193	0.030277
5	0.0307	0.012812	0.014045	0.026856
6	0.0159	0.009488	0.018571	0.030779
7	0.0263	0.009856	0.0128	0.026856
8	0.0864	0.009345	0.01004	0.019384
9	0.0325	0.01003	0.009895	0.019926
10	0.0325	0.013448	0.007022	0.020471
11	0.0562	0.005331	0.009317	0.014647
12	0.0244	0.026253	0.031952	0.058205
Average	0.037	0.013008	0.016325	0.02855
Stdev	0.018244	0.005385	0.010325	0.014892

5. Concusion

The main question of this thesis is whether it is possible to have two-phase steady-state flow through a two-dimensional microfluidic network. In Hadjisotiriou (2020) is has been established that two-phase flow paths could co-exist within a 32x32 network with the use of liquid bridges, but only a relatively small amount of water will flow compared to the amount of gas. With the estimate calculated there would be around 66 times more gas than water flowing through the networks at approximately equal pore throat occupancy. This result is more realistic than previously obtained in Hadjisotiriou (2020).

6. Discussion

Not all the water flow paths are taken into account; in that sense the estimate of water conductivity may be an underestimate. However, both the horizontal and vertical flow paths have been used in determining the equivalent resistance of the water network. This roughly doubles the conductivity from what it would be for flow in either direction. Moreover, we assumed zero resistance in flow through water-filled pores and throats, and that all counted water flow paths are in parallel, while in reality they share (and compete for flow in) some segments. Those factors would tend to give an overestimate of liquid conductivity.

In determining the equivalent resistance value of the whole gas network, the resistance values of the gas flowing through a liquid bridge have not been used in the calculations. But the liquid bridges are also shaped very generously towards the water flow which might compensate for it.

Also, the cylindrical pillars with this distance between them appear to help to stabilize bridges greatly according to Cox (2020). If the network was shaped differently liquid bridges might not be able to form at all.

The larger implications of this result are as follows:

Foam stability, once foam is created, is very sensitive to the capillary pressure (Rossen, 1996)., In the networks illustrated in Appendix B water saturation is close to 50%. For saturations below this, water cannot flow out of the network to reduce water to lower saturations. This makes it hard to raise the capillary pressure to levels at which foam stability is at issue. This in turn makes it difficult to explore foam stability in a microfluidic device. (Rossen, 2020)

During waterflooding oil is trapped inside the 3D porous media, and liberating it requires extraordinarily large pressure gradient or extremely low interfacial tension. Those are exceptional circumstances in 3D geological porous media. In a microfluidic device, there is no two-phase flow unless one is at high enough capillary number to allow both phases to flow as discontinuous phases. This is not representative of rock pore space. (Rossen, 2020)

7. Relation of the thesis to the Applied Earth Sciences

The topic of this thesis furthers the understanding of flow processes in porous media. This of importance to several industries.

Hydrocarbon energy
The production rate of the hydrocarbon industry is highly dependent on understanding these processes well. The industry is under discussion a lot recently. But we still have a society which is substantially reliant on hydrocarbons for several decades at least. Of nearly everything consumed or used, oil or gas is used directly. If not it is used in its manufacturing or its transport. (Blunt, 2020)

Geothermal energy
Due to the recent focus on increasing the supply of renewable energy, it calls attention to re-evaluating all the alternative energy sources, including the use of geothermal energy. Conventional hydrothermal resources are already in use for electric and non-electric applications, but are limited by their locations. Enhanced Geothermal Systems (EGS) are resources with great potential for primary energy recovery using heat-mining technology. It is also possible to use the hot water coproduced with oil and gas production, or to tap into geopressured resources that contain hot water with methane dissolved in it (Tester et al., 2006).

Carbon Capture and Storage
CCS could potentially facilitate the net removal of CO_2 of the atmosphere. Carbon capture and subsequent storage in porous geological formations has the potential to grow into an industry as large the oil and gas industry. (Blunt, 2020) But despite a broad positive consensus and the technical maturity, it has not been deployed at a scale in line with the decade old ambitions. (Mai & Macdowell, 2020).

Groundwater use and protection
Groundwater is essential for human health, food security, energy and ecosystems. It is by far the

largest source of freshwater (Gleeson, T., Befus, K., Jasechko, S. et al., 2016). The demographic increase in the world and increase in water demand creates problems for the groundwater systems in less-developed countries. The groundwater systems must be understood better to create meaningful policies for sustainable development and protection of the groundwater reserves (Danielopol et al., 2003).

Foams

Foams are used in enhanced oil recovery (EOR), which is part of reservoir engineering (Rossen, 1996).

Foams are used in EOR to increase sweep across heterogeneous layered reservoirs. In environmental remediation, they are used to prevent the spread of contaminants. In carbon storage, they are used to increase capillary trapping.

To enhance oil recovery gasses are injected into reservoirs to increase the production and recovery rate. During this process, gas breakthrough could occur which means that the gas will not be able to reach large parts of the reservoir. This happens when preferential gas flow paths towards the production well occur; these reduce the sweep efficiency and result in a high produced gas/oil ratio (Rossen, 1996). A gas breakthrough could happen because of high permeability zones named thief zones, viscous fingering or gravitational segregation (Rognmo, 2018).

Foams are used to combat the loss of sweep efficiency by a reduction of gas mobility and diverting fluids to another less permeable part of the reservoir. This happens because the foams plug up the zones with higher permeability. The surfactant stabilizes the liquid lamellae, resulting in better foam generation and reduction of gas mobility (Almajid & Kovscek, 2019; Rossen, 1996)

With the plugging and diversion possible using a relatively small amount of foam near an injection or a production well, the sweep efficiency of the injected gasses may already increase. In other cases the effect might be localized around the well and have little effect on the bulk of the flow patterns throughout the reservoir. In the case of the production well it might be sufficient to prevent unwanted fluids and gasses from entering the well. The foam type used for plugging has to have zero mobility ideally, be stable for a long time but capable of being destroyed if neede. (Rossen, 1996).

The technique that has more effect on the flow patterns throughout the whole formation is named “mobility control”. It improves the oil recovery greatly but also takes a much longer time to achieve. The foam type used for mobility control has to be able to propagate rapidly, but with low mobility. The rheology of the foam should be shear-thinning so that the viscosity decreases under shear strain which aids the injectivity (Rossen, 1996).

A. Bibliography

Almajid, M. M., & Kovscek, A. R. (2019). Pore Network Investigation of Trapped Gas and Foam Generation Mechanisms. Transport in Porous Media, 131(1), 289–313. https://doi.org/10.1007/s11242-018-01224-4

Blunt, M. J. (2020). Flow in Porous Materials (GeoScience & GeoEnergy Webinar 23 April 2020).

Gleeson, T., Befus, K., Jasechko, S. et al. (2016)The global volume and distribution of modern groundwater. Nature Geosci 9, 161–167. https://doi.org/10.1038/ngeo2590

Hadjisotiriou, G. (2020). Fluid Conductivity of Steady Two-Phase Flow in a 2D Micromodel: Analysis of a Representative 2D Percolation Model (Bachelor End Project). Delft, Netherlands: TU Delft.

Holstvoogd, J. (2020). Analysis of Steady Multiphase Flow in Porous Media: Across a Hypothetical 2D Percolating Network (Bachelor End Project). Delft, Netherlands: TU Delft.

Hunt, A. G., & Sahimi, M. (2017). Flow, Transport, and Reaction in Porous Media: Percolation Scaling, Critical-Path Analysis, and Effective Medium Approximation. Reviews of Geophysics, 55(4), 993–1078. https://doi.org/10.1002/2017rg000558

Kovscek, A. R., Tang, G.-Q., & Radke, C. J. (2007). Verification of Roof snap off as a foam-generation mechanism in porous media at steady state. Colloids and Surfaces A: Physicochemical and Engineering Aspects, 302(1–3), 251–260. https://doi.org/10.1016/j.colsurfa.2007.02.035

Mai, B., & MacDowell, N. (2020). Introduction. In Carbon capture and storage (pp. 1-7). Cambridge: Royal Society of Chemistry.

Ransohoff, T. C., & Radke, C. J. (1988). Laminar flow of a wetting liquid along the corners of a predominantly gas-occupied noncircular pore. Journal of Colloid and Interface Science, 121(2), 392–401. https://doi.org/10.1016/0021-9797(88)90442-0

Rognmo, A. U. (2018). CO2-Foams for Enhanced Oil Recovery and CO2 Storage. Retrieved from https://www.researchgate.net/publication/332158061_CO2-Foams_for_Enhanced_Oil_Recovery_and_CO2_Storage

Rossen, W. R. (1996). Foams in enhanced oil recovery. In R. K. Prud'homme & S. A. Khan (Eds.), Foams theory, measurements, and applications (pp. 413–445). New York, USA: Marcel Decker, inc.

Rossen, W. R. (2003). A critical review of Roof snap-off as a mechanism of steady-state foam generation in homogeneous porous media. Colloids and Surfaces A: Physicochemical and Engineering Aspects, 225(1–3), 1–24. https://doi.org/10.1016/s0927-7757(03)00309-1

Rossen, W. R. (2008). Comment on "Verification of Roof snap-off as a foam-generation mechanism in porous media at steady state." Colloids and Surfaces A: Physicochemical and Engineering Aspects, 322(1–3), 261–269. https://doi.org/10.1016/j.colsurfa.2008.02.034

Rossen, W. R. (2020). E-mail correspondence

Tester, J. W. (2007) The Future of Geothermal Energy, Cambridge, MA: Massachusetts Institute of Technology

Danielopol, D. L., Griebler, C., Gunatilaka, A., & Notenboom, J. (2003). Present state and future prospects for groundwater ecosystems [Abstract]. Environmental Conservation, 30(2), 104-130. doi:10.1017/s0376892903000109

B. Appendix

B1. Slip and no-slip flow rates and resistances of H_2O, CO_2, and N_2 through all the geometries.

Table 3: Slip, H_2O

	Q [m^3/s]	1/Q	R
R1	7.31E-18	1.37E+17	7.75
R2	3.72E-18	2.69E+17	15.23
Rb 1	1.78E-18	5.61E+17	31.80
Rb 2	2.39E-18	4.19E+17	23.75
Rb 3	3.30E-18	3.03E+17	17.16
Rb 4	3.26E-18	3.06E+17	17.35
Rg	5.67E-17	1.77E+16	1.00
Rgb	2.27E-17	4.41E+16	2.50

Table 4: No slip, H_2O

	Q [m^3/s]	1/Q	R
R1	5.99E-18	1.67E+17	9.45
R2	2.42E-18	4.13E+17	23.37
Rb 1	1.18E-18	8.47E+17	47.99
Rb 2	1.71E-18	5.84E+17	33.06
Rb 3	2.77E-18	3.61E+17	20.45
Rb 4	2.74E-18	3.65E+17	20.68
Rg	5.67E-17	1.77E+16	1.00
Rgb	2.27E-17	4.41E+16	2.50

Table 5: Slip, CO_2

	Q [m^3/s]	1/Q	R
R1	7.31E-18	1.37E+17	532.45
R2	3.72E-18	2.69E+17	1046.79
Rb 1	1.78E-18	5.61E+17	2185.25
Rb 2	2.39E-18	4.19E+17	1631.79
Rb 3	3.30E-18	3.03E+17	1179.28
Rb 4	3.26E-18	3.06E+17	1192.54
Rg	3.89E-15	2.57E+14	1.00
Rgb	1.56E-15	6.41E+14	2.50

Table 6: No slip, CO_2

	Q [m^3/s]	1/Q	R
R1	5.99E-18	1.67E+17	649.53
R2	2.42E-18	4.13E+17	1606.01
Rb 1	1.18E-18	8.47E+17	3297.87
Rb 2	1.71E-18	5.84E+17	2271.84
Rb 3	2.77E-18	3.61E+17	1405.39
Rb 4	2.74E-18	3.65E+17	1420.89
Rg	3.89E-15	2.57E+14	1.00
Rgb	1.56E-15	6.41E+14	2.50

Table 7: Slip, N_2

	Q [m^3/s]	1/Q	R
R1	7.31E-18	1.37E+17	448.55
R2	3.72E-18	2.69E+17	881.84
Rb 1	1.78E-18	5.61E+17	1840.91
Rb 2	2.39E-18	4.19E+17	1374.66
Rb 3	3.30E-18	3.03E+17	993.46
Rb 4	3.26E-18	3.06E+17	1004.63
Rg	3.28E-15	3.05E+14	1.00
Rgb	1.31E-15	7.61E+14	2.50

Table 8: No slip, N_2

	Q [m^3/s]	1/Q	R
R1	5.99E-18	1.67E+17	547.18
R2	2.42E-18	4.13E+17	1352.94
Rb 1	1.18E-18	8.47E+17	2778.21
Rb 2	1.71E-18	5.84E+17	1913.86
Rb 3	2.77E-18	3.61E+17	1183.94
Rb 4	2.74E-18	3.65E+17	1196.99
Rg	3.28E-15	3.05E+14	1.00
Rgb	1.31E-15	7.61E+14	2.50

B2. Pressure and Velocity profiles

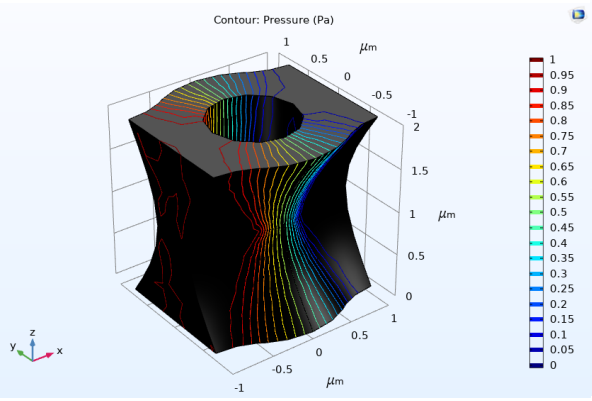

Figure 26A: R1, no-slip, H_2O, pressure profile.

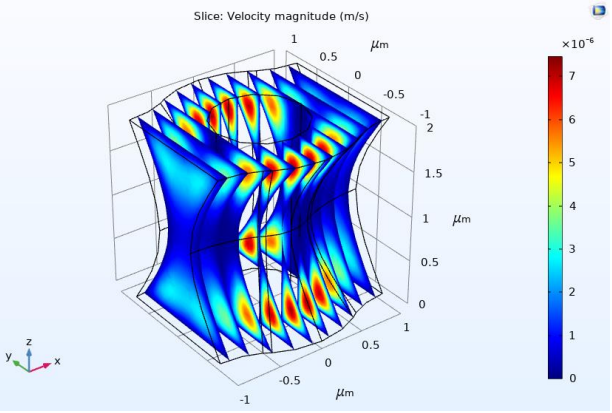

Figure 26B: R1, no-slip, H_2O, velocity profile.

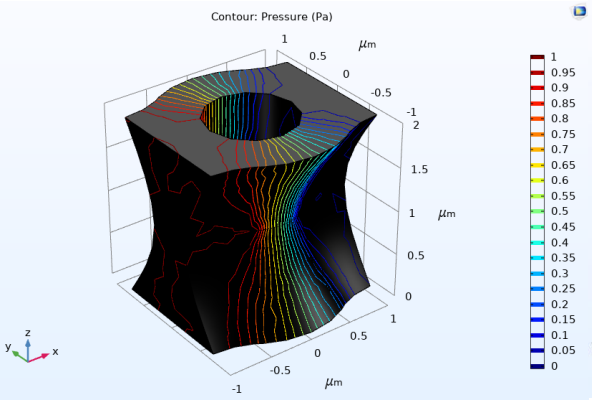

Figure 27A: R1, slip, H_2O, pressure profile.

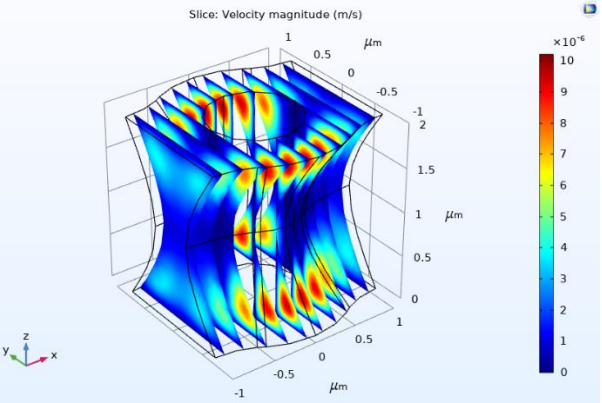

Figure 27B: R1, slip, H_2O, velocity profile.

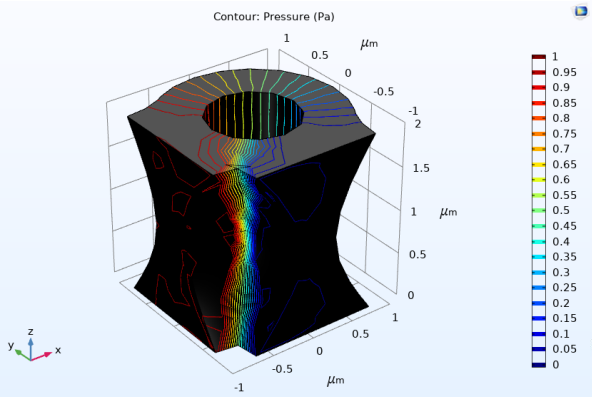

Figure 28A: R2, no-slip, H_2O, pressure profile.

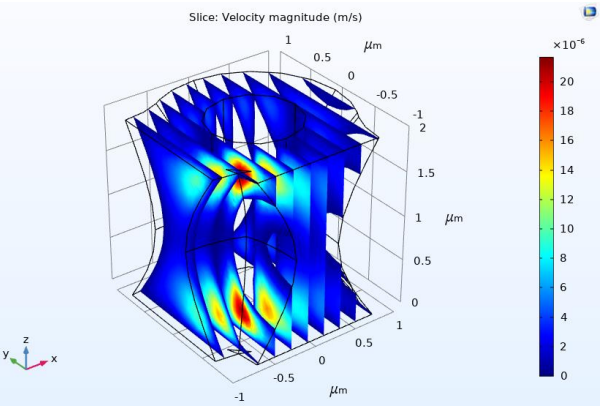

Figure 28B: R2, no-slip, H_2O, velocity profile.

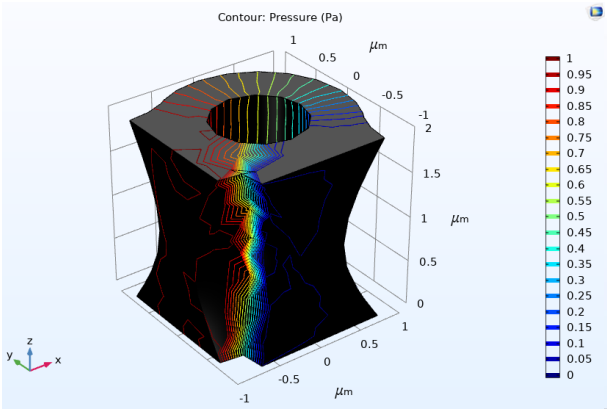

Figure 29A: R2, slip, H_2O, pressure profile.

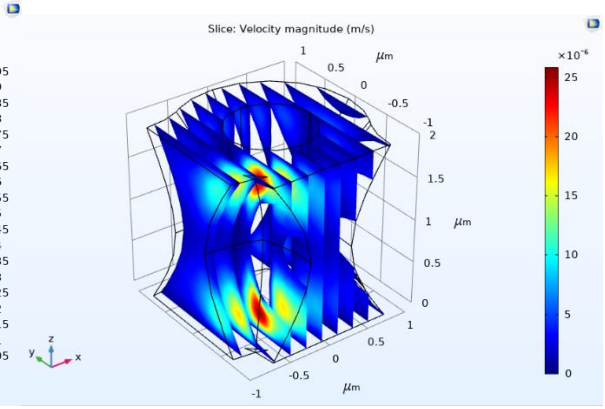

Figure 29B: R2, slip, H_2O, velocity profile.

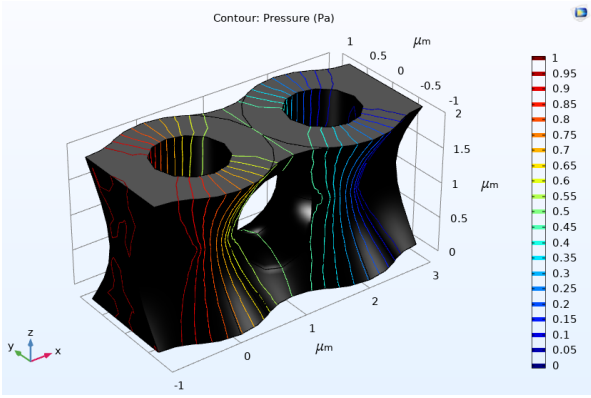

Figure 30A: Rb1, no-slip, H_2O, pressure profile.

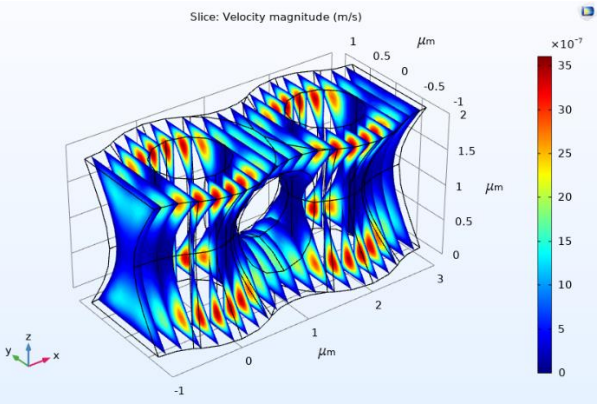

Figure 30B: Rb1, no-slip, H_2O, velocity profile.

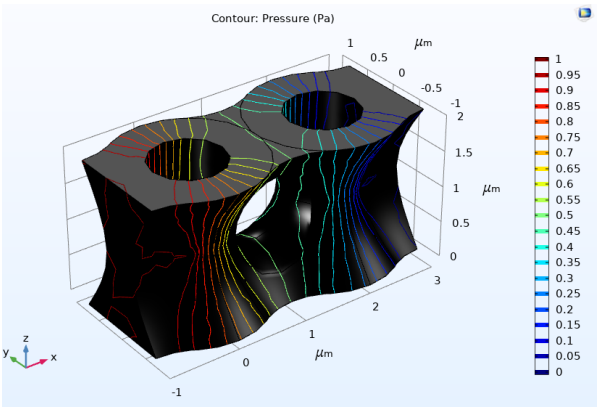

Figure 31A: Rb1, slip, H_2O, pressure profile.

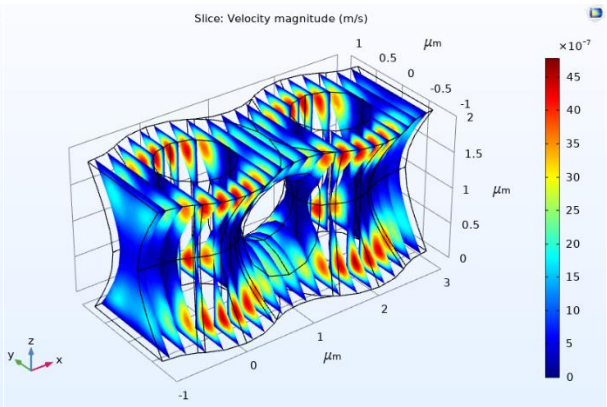

Figure 31B: Rb1, slip, H_2O, velocity profile.

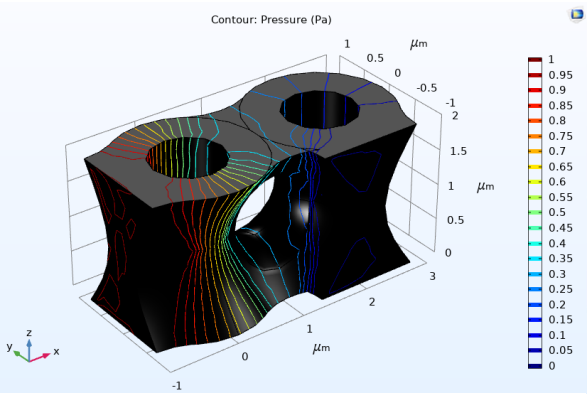

Figure 32A: Rb2, no-slip, H_2O, pressure profile.

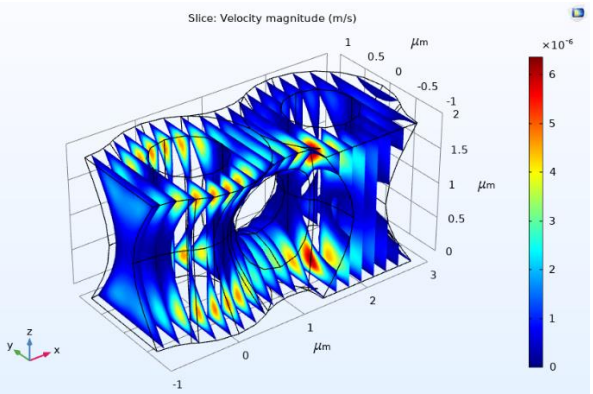

Figure 32B: Rb2, no-slip, H_2O, velocity profile.

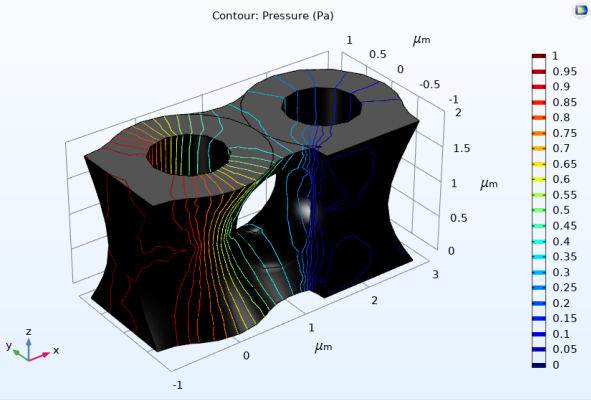

Figure 33A: Rb3, slip, H_2O, pressure profile.

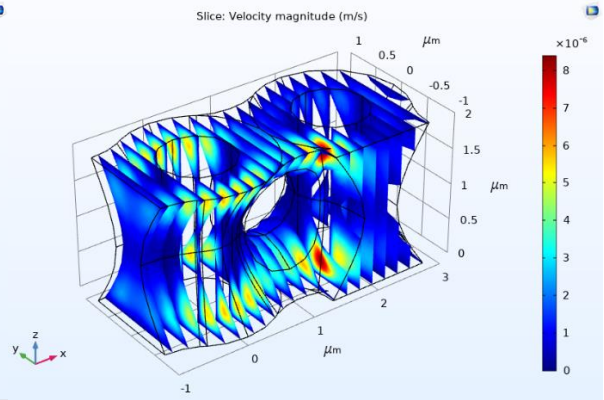

Figure 33B: Rb3, slip, H_2O, velocity profile.

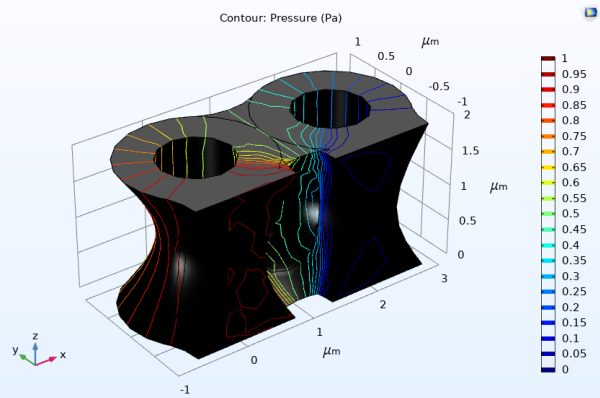

Figure 34A: Rb3, no-slip, H_2O, pressure profile.

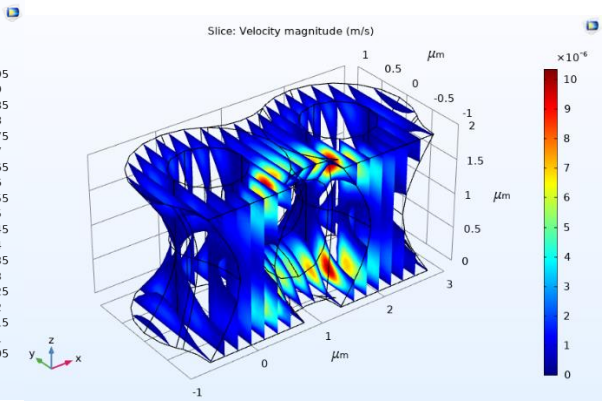

Figure 34B: Rb3, no-slip, H_2O, velocity profile.

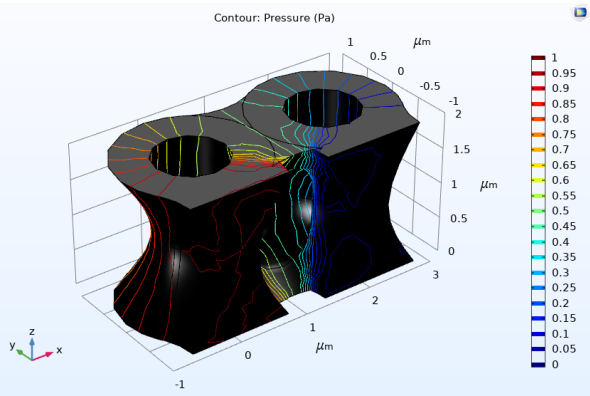

Figure 35A: Rb3, slip, H_2O, pressure profile.

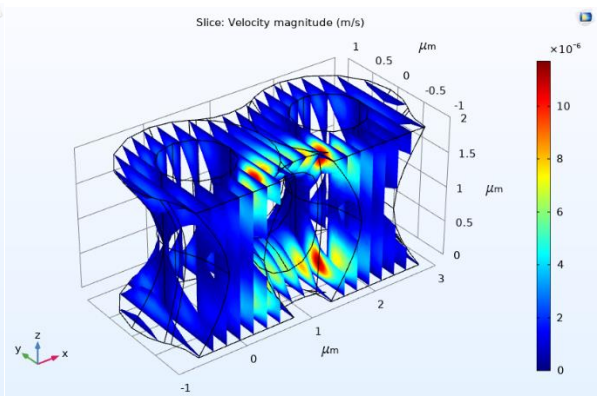

Figure 35B: Rb3, slip, H_2O, velocity profile.

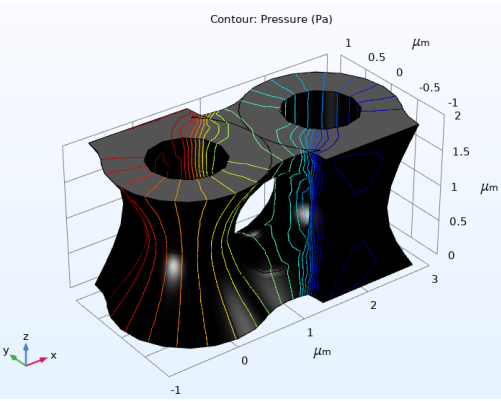

Figure 36A: Rb4, no-slip, H_2O, pressure profile.

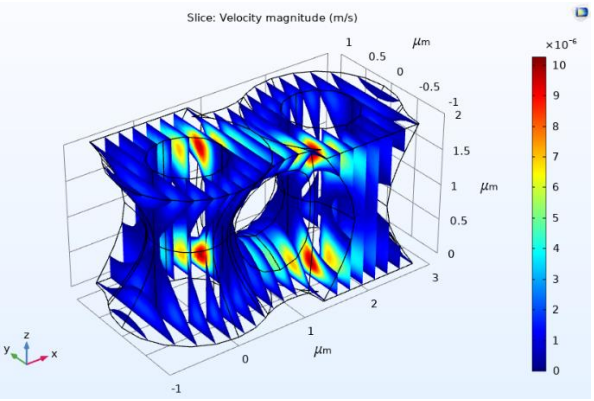

Figure 36B: Rb4, no-slip, H_2O, velocity profile.

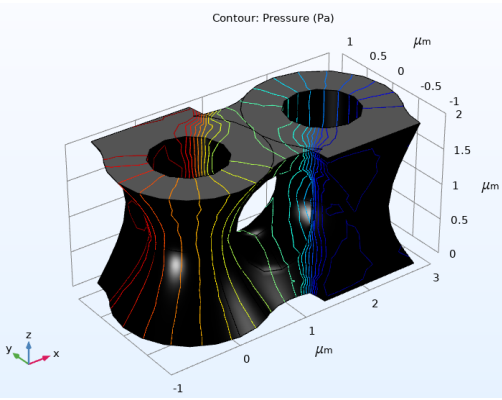

Figure 37A: Rb4, slip, H_2O, pressure profile.

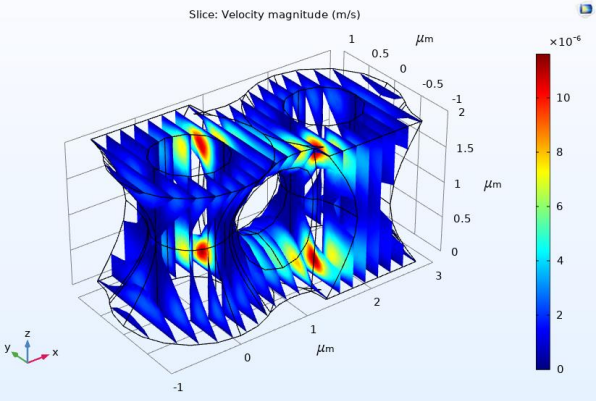

Figure 37B: Rb4, slip, H_2O, velocity profile.

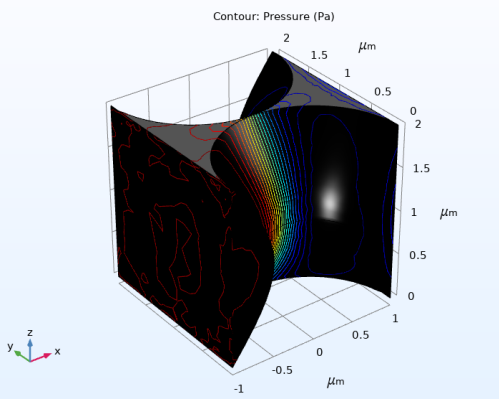

Figure 38A: Rg, no-slip, H_2O, pressure profile.

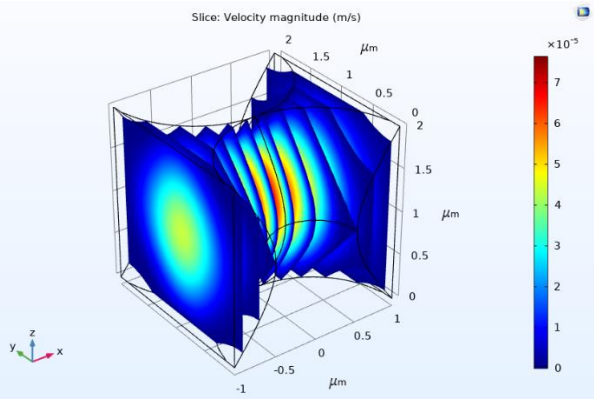

Figure 38B: Rg, no-slip, H_2O, velocity profile.

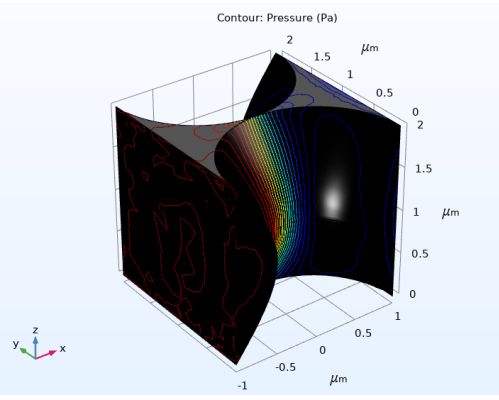

Figure 39A: Rg, no-slip, CO_2, pressure profile.

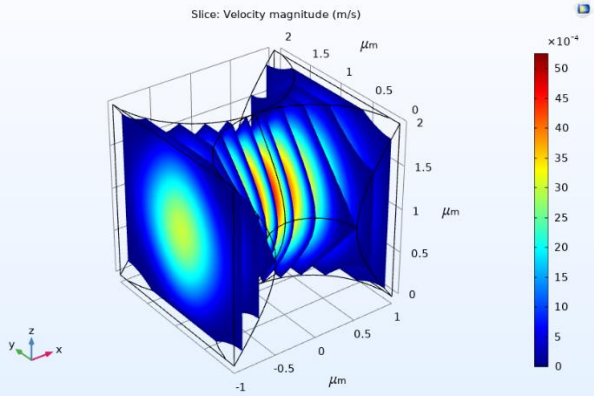

Figure 39B: Rg, no-slip, CO_2, velocity profile.

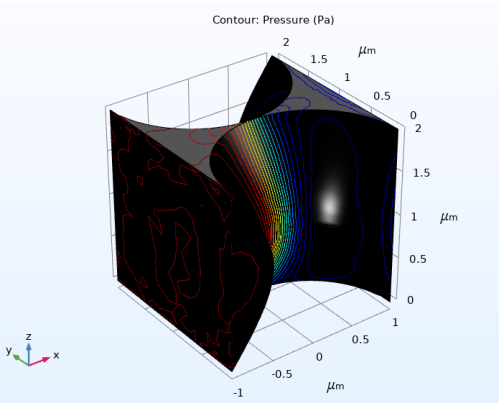

Figure 40A: Rg, no-slip, N_2, pressure profile.

Figure 40B: Rg, no-slip, N_2, velocity profile.

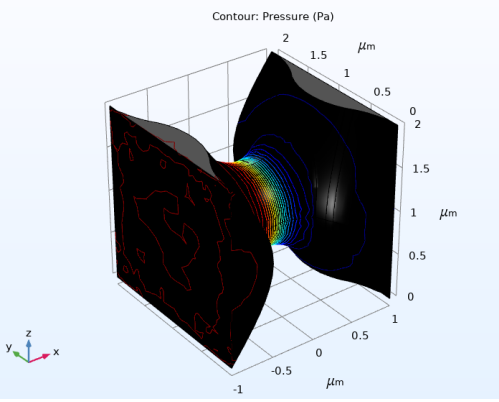

Figure 41A: Rgb, no-slip, H_2O, pressure profile.

Figure 41B: Rgb, no-slip, H_2O, velocity profile.

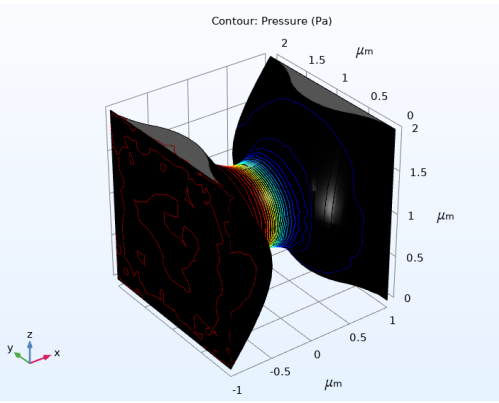

Figure 42A: Rgb, no-slip, CO_2, pressure profile.

Figure 42B: Rgb, no-slip, CO_2, velocity profile.

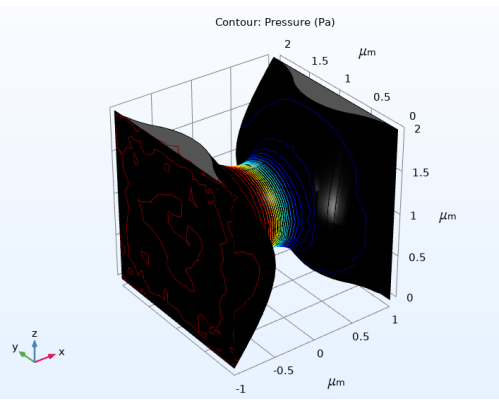

Figure 43A: Rgb, no-slip, N_2, pressure profile.

Figure 43B: Rgb, no-slip, N_2, velocity profile.

B3. Hadjisotiriou (2020) Networks

"The liquid paths and their corresponding conductivity data are presented per network in the right column. The gas conductivity graphs are given in the left column and their minor gas paths are highlighted in neon green." (Hadjisotiriou, 2020)

Two counts of R1 have been removed per Rb in the water flow path as those overlapped before.

The amount of bridges has been counted in the work of Hadjisotiriou, but the four different bridge shapes have not been considered. So instead of recounting the bridges, the resistance value of Rb3 is chosen because it is the most favorable towards the water flow.

Network 1 (p=0,50)

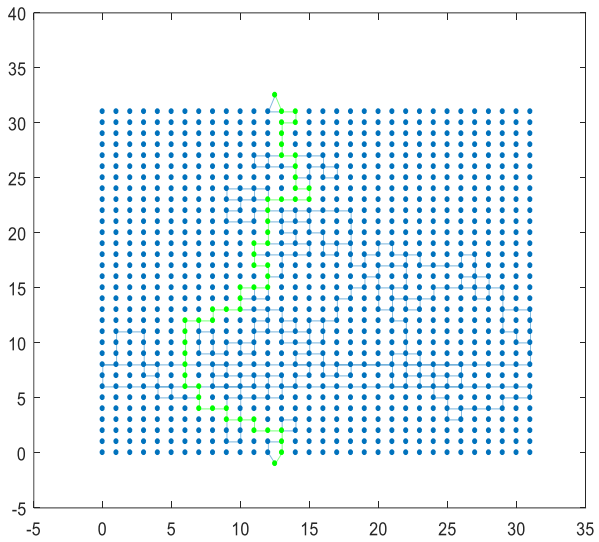

Figure 44: The shortest gas path in green, the gas backbone in blue.

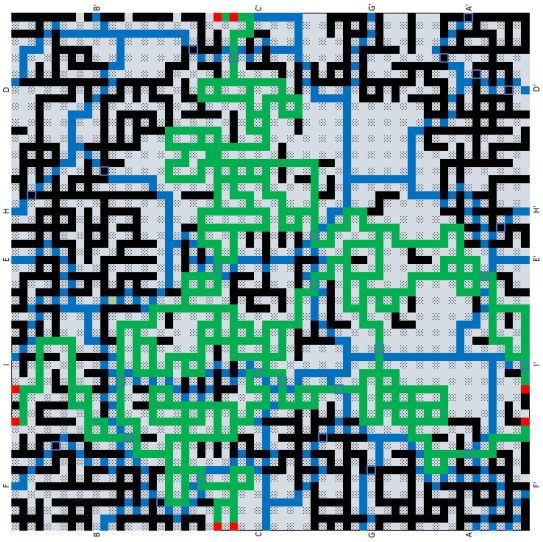

Figure 45: The water and gas paths.

Table 9: The total conductivity of the gas network is given by C gas in Hadjisotiriou. The resistance of the gas network is given by R gas. The tables show the counts for the flow geometries and the total resistance per flow path. To the right of the tables the total resistance for the horizontal and vertical directions are given for both the slip and no slip conditions.

C gas	R gas							
0.0303	33.0033							
Horizontal							All Horizontal paths	
	R1	R1 corrected	R2	Rb	R Slip	R No Slip	R slip	R no slip
DD'	26	24	2	1	233.59	294.05	59.67029	75.44653
II'	25	19	2	3	229.17	287.69		
FF'	32	28	4	2	312.21	399.05		
EE'	43	41	4	1	395.78	501.48		
HH'	43	31	5	6	419.34	532.59		
Vertical							All Vertical paths	
	R1	R1 corrected	R2	Rb	R Slip	R No Slip	R slip	R no slip
CC'	38	36	6	1	387.51	500.96	99.03226	126.3247
GG'	37	31	5	3	367.85	471.23		
BB'	45	41	4	2	412.94	521.93		
AA'	46	42	4	2	420.69	531.38		

Network 2 (p=0,51)

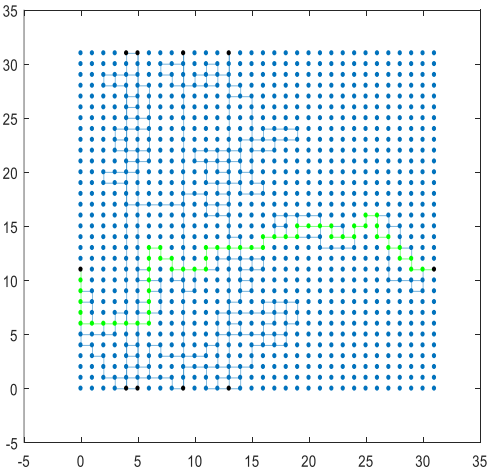

Figure 46: The shortest gas path in green, the gas backbone in

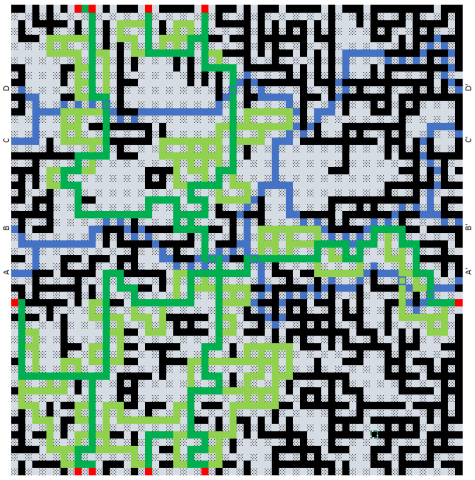

Figure 47: The water and gas paths.

Table 10: The total conductivity of the gas network is given by C gas in Hadjisotiriou. The resistance of the gas network is given by R gas. The tables show the counts for the flow geometries and the total resistance per flow path. To the right of the tables the total resistance for the horizontal and vertical directions are given for both the slip and no slip conditions.

C gas	R gas							
0.0341	29.3255132							
Horizontal							All Horizontal paths	
	R1		R1 Corrected	R2	Rb	R Slip	R No Slip	R slip	R no slip
AA'		42	38	5	2	404.93	516.95	90.00636	117.6974
BB'		33	31	5	1	333.53	430.33		
CC'		27	21	9	3	351.30	470.20		
DD'		30	26	8	2	357.65	473.63		

Network 3 (p=0,51)

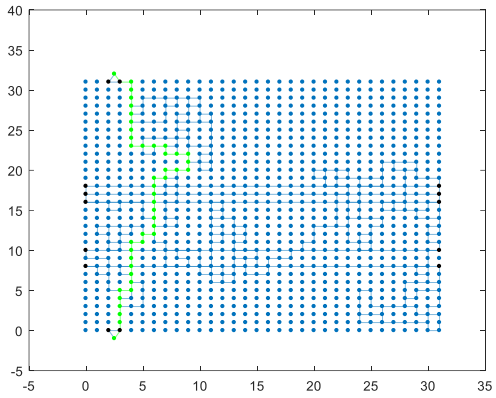

Figure 48: The shortest gas path in green, the gas backbone in

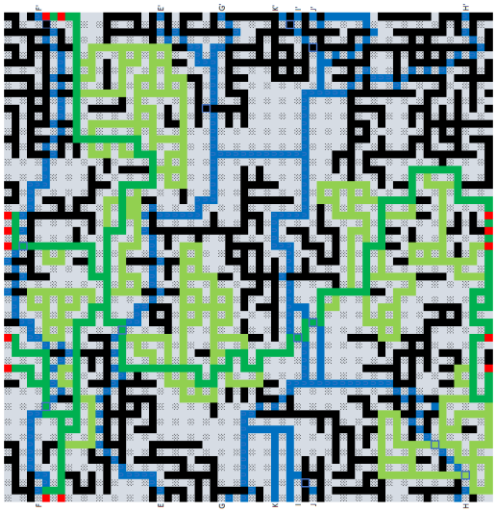

Figure 49: The gas backbone and the first half of the water flow

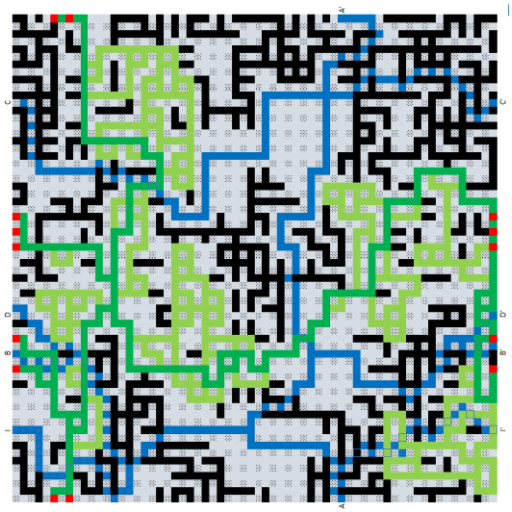

Figure 50: The gas backbone and the second half of the water flow paths.

Table 11: The total conductivity of the gas network is given by C gas in Hadjisotiriou. The resistance of the gas network is given by R gas. The tables show the counts for the flow geometries and the total resistance per flow path. To the right of the tables the total resistance for the horizontal and vertical directions are given for both the slip and no slip conditions.

C gas	R gas
0.0375	26.66667

Horizontal							All Horizontal paths	
	R1	R1	R2	Rb	R Slip	R No Slip	R slip	R no slip
II'	11	7	2	2	119.03	153.81	56.87941	73.82996
CC'	23	21	7	1	286.51	382.55		
DD'	35	31	5	2	350.69	450.78		
BB'	35	29	5	3	352.36	452.33		

Vertical							All Vertical paths	
	R1	R1	R2	Rb	R Slip	R No Slip	R slip	R no slip
AA'	19	17	2	1	179.35	227.88	25.22247	31.85366
EE'	24	20	8	2	311.16	416.92		
FF'	34	28	5	3	344.61	442.88		
GG'	16	12	2	2	157.77	201.07		
HH'	33	27	6	3	352.09	456.79		
II'	33	19	1	7	282.59	346.13		
JJ'	16	12	3	2	173.01	224.44		
KK'	13	7	0	3	105.72	127.52		

Network 4 (p=0,51)

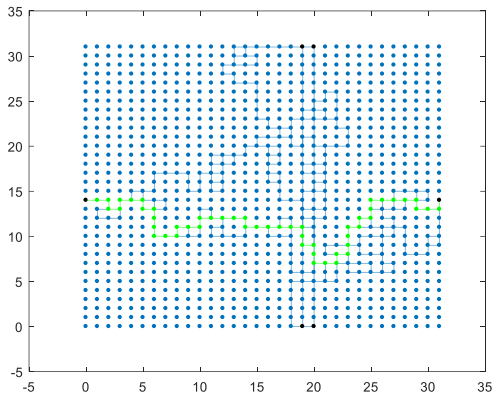

Figure 51: The shortest gas path in green, the gas backbone in

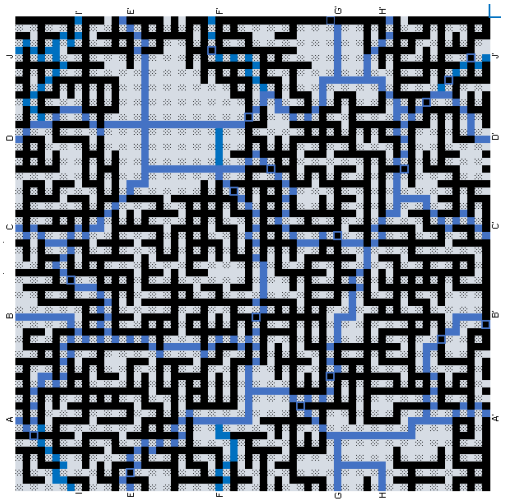

Figure 52: The water flow paths.

Table 12: The total conductivity of the gas network is given by C gas in Hadjisotiriou. The resistance of the gas network is given by R gas. The tables show the counts for the flow geometries and the total resistance per flow path. To the right of the tables the total resistance for the horizontal and vertical directions are given for both the slip and no slip conditions.

C gas	R gas							
0.0372	26.88172							
Horizontal							All Horizontal paths	
						R No		
	R1	R1	R2	Rb	R Slip	Slip	R slip	R no slip
DD'	25	21	1	2	212.27	262.77	71.00322	88.57623
CC'	28	20	4	4	284.55	364.34		
BB'	41	37	2	2	351.48	437.38		
AA'	40	32	1	4	331.83	407.65		
Vertical							All Vertical paths	
						R No		
	R1	R1	R2	Rb	R Slip	Slip	R slip	R no slip
FF'	31	25	5	3	321.36	414.52	61.75473	79.87237
EE'	29	23	6	3	321.10	418.99		
GG'	30	28	8	1	355.99	472.09		
HH'	28	20	8	4	345.48	457.82		
II'	50	46	5	2	466.92	592.56		
JJ'	58	50	1	4	471.30	577.79		

Network 5 (p=0,52)

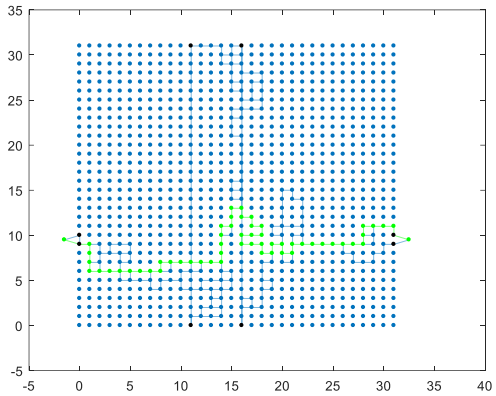

Figure 53: The shortest gas path in green, the gas backbone in

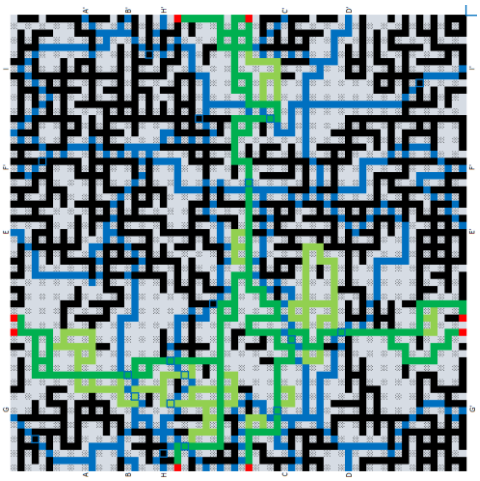

Figure 54: The water and gas paths.

Table 13 The total conductivity of the gas network is given by C gas in Hadjisotiriou. The resistance of the gas network is given by R gas. The tables show the counts for the flow geometries and the total resistance per flow path. To the right of the tables the total resistance for the horizontal and vertical directions are given for both the slip and no slip conditions.

C gas	R gas							
0.0307	32.57329							
Horizontal							All Horizontal paths	
	R1	R1	R2	Rb	R Slip	R No Slip	R slip	R no slip
EE'	43	41	4	1	395.78	501.48	78.05456	99.02863
FF'	32	28	4	2	312.21	399.05		
GG'	37	31	5	3	367.85	471.23		
II'	25	19	2	3	229.17	287.69		
Vertical							All Vertical paths	
	R1	R1	R2	Rb	R Slip	R No Slip	R slip	R no slip
AA'	46	42	4	2	420.69	531.38	71.20009	90.31435
BB'	45	41	4	2	412.94	521.93		
CC'	38	36	6	1	387.51	500.96		
DD'	26	24	2	1	233.59	294.05		
HH'	43	31	5	6	419.34	532.59		

Network 6 (p=0,52)

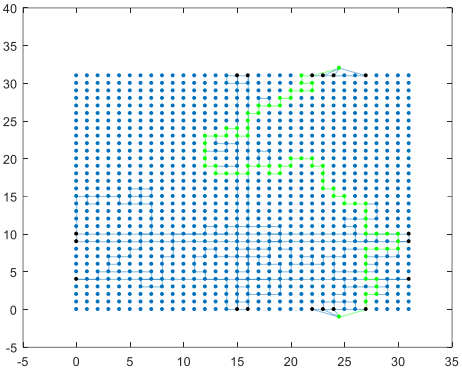

Figure 55: The shortest gas path in green, the gas backbone in

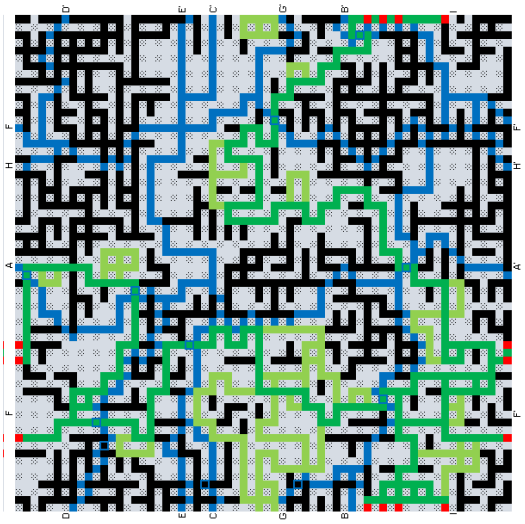

Figure 56: The water and gas paths.

Table 14: The total conductivity of the gas network is given by C gas in Hadjisotiriou. The resistance of the gas network is given by R gas. The tables show the counts for the flow geometries and the total resistance per flow path. To the right of the tables the total resistance for the horizontal and vertical directions are given for both the slip and no slip conditions.

C gas	R gas							
0.0159	62.89308							
Horizontal							All Horizontal paths	
	R1	R1	R2	Rb	R Slip	R No Slip	R slip	R no slip
AA'	30	24	3	3	283.15	358.32	105.4	132.9608
FF'	36	34	2	1	311.08	388.57		
HH'	39	37	4	1	364.79	463.67		
Vertical								
	R1	R1	R2	Rb	R Slip	R No Slip	All Vertical paths	
BB'	35	29	6	3	367.59	475.70	R slip	R no slip
CC'	15	11	1	2	134.79	168.25	53.84734	67.21199
DD'	42	38	2	2	359.23	446.83		
EE'	19	17	1	1	164.12	204.51		
GG'	48	40	4	4	439.52	553.38		

Network 7 (p=0,51)

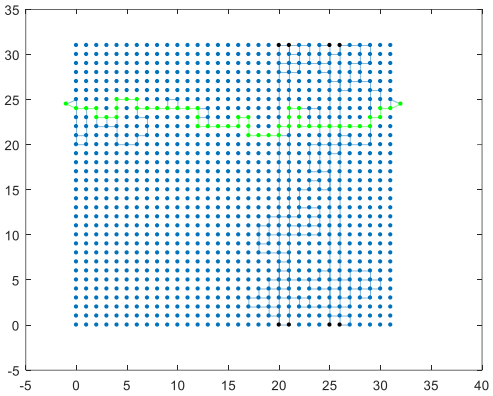

Figure 57: The shortest gas path in green, the gas backbone in

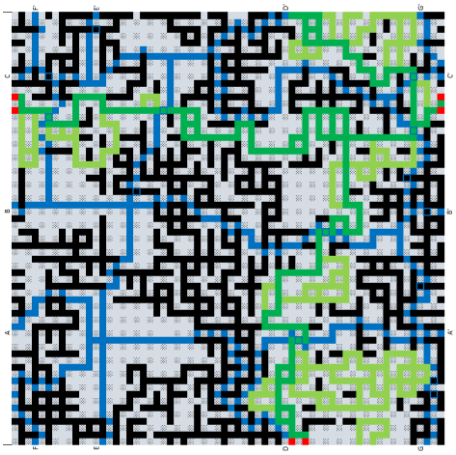

Figure 58: The water and gas paths.

Table 15: The total conductivity of the gas network is given by C gas in Hadjisotiriou. The resistance of the gas network is given by R gas. The tables show the counts for the flow geometries and the total resistance per flow path. To the right of the tables the total resistance for the horizontal and vertical directions are given for both the slip and no slip conditions.

C gas	R gas							
0.0864	11.57407							
Horizontal							All Horizontal paths	
	R1	R1	R2	Rb	R Slip	R No Slip	R slip	R no slip
BB'	42	32	8	5	455.63	591.70	107.0112	136.5442
EE'	42	36	6	3	421.83	541.86		
FF'	53	43	3	5	464.69	578.82		
HH'	38	26	5	6	380.60	485.33		
Vertical							All Vertical paths	
	R1	R1	R2	Rb	R Slip	R No Slip	R slip	R no slip
AA'	49	41	5	4	462.50	586.21	99.60626	127.323
CC'	43	35	6	4	431.24	552.86		
DD'	32	24	5	4	330.78	425.52		
GG'	40	30	5	5	394.43	502.68		

Network 8 (p=0,48)

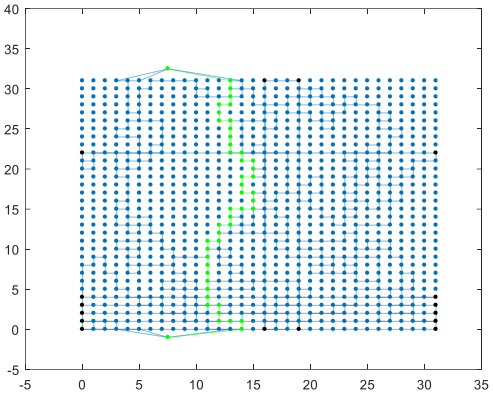

Figure 59: The shortest gas path in green, the gas backbone in

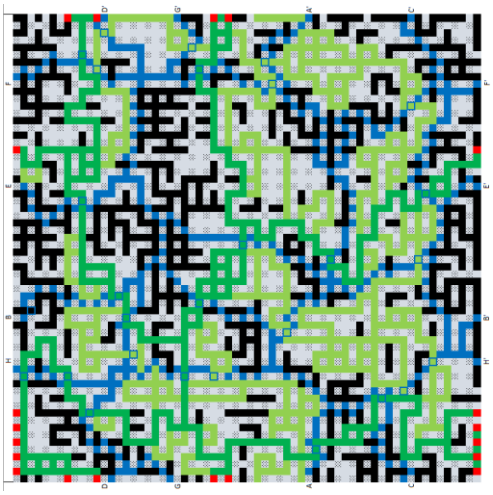

Figure 60: The water and gas paths.

Table 16: The total conductivity of the gas network is given by C gas in Hadjisotiriou. The resistance of the gas network is given by R gas. The tables show the counts for the flow geometries and the total resistance per flow path. To the right of the tables the total resistance for the horizontal and vertical directions are given for both the slip and no slip conditions.

C gas	R gas							
0.0864	11.57407							
Horizontal							All Horizontal paths	
	R1		R1	R2	Rb	R Slip	R No Slip	R slip	R no slip
BB'		42	32	8	5	455.63	591.70	107.0112	136.5442
EE'		42	36	6	3	421.83	541.86		
FF'		53	43	3	5	464.69	578.82		
HH'		38	26	5	6	380.60	485.33		
Vertical							All Vertical paths	
	R1		R1	R2	Rb	R Slip	R No Slip	R slip	R no slip
AA'		49	41	5	4	462.50	586.21	99.60626	127.323
CC'		43	35	6	4	431.24	552.86		
DD'		32	24	5	4	330.78	425.52		
GG'		40	30	5	5	394.43	502.68		

Network 9 (p=0,47)

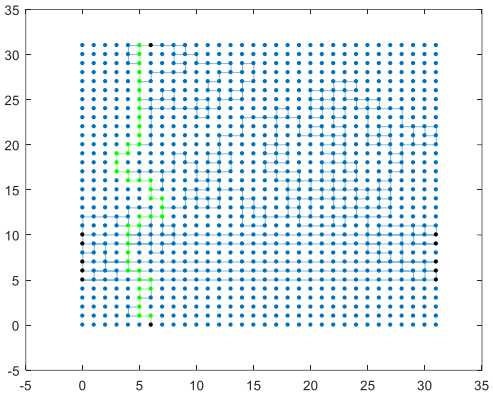

Figure 61: The shortest gas path in green, the gas backbone in

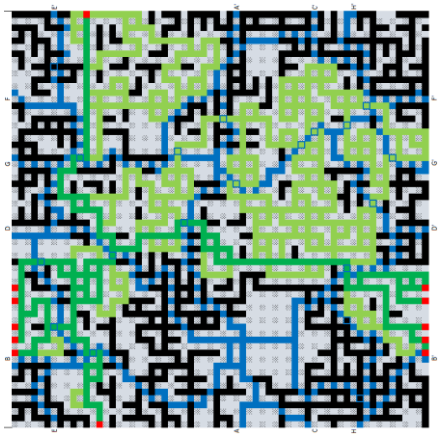

Figure 62: The water and gas paths.

Table 17: The total conductivity of the gas network is given by C gas in Hadjisotiriou. The resistance of the gas network is given by R gas. The tables show the counts for the flow geometries and the total resistance per flow path. To the right of the tables the total resistance for the horizontal and vertical directions are given for both the slip and no slip conditions.

C gas	R gas							
0.0325	30.76923							
Horizontal							All Horizontal paths	
	R1	R1	R2	Rb	R Slip	R No Slip	R slip	R no slip
BB'	35	31	4	2	335.46	427.41	99.69634	129.5642
DD'	36	32	7	2	388.91	506.98		
FF'	41	39	11	1	486.92	646.17		
GG'	36	22	8	7	412.46	538.08		
Vertical							All Vertical paths	
	R1	R1	R2	Rb	R Slip	R No Slip	R slip	R no slip
AA'	32	28	6	2	342.68	445.79	101.0594	129.7845
CC'	37	33	7	2	396.66	516.43		
EE'	44	38	3	3	391.63	490.65		
HH'	53	43	7	5	525.63	672.31		

Network 10 (p=0,45)

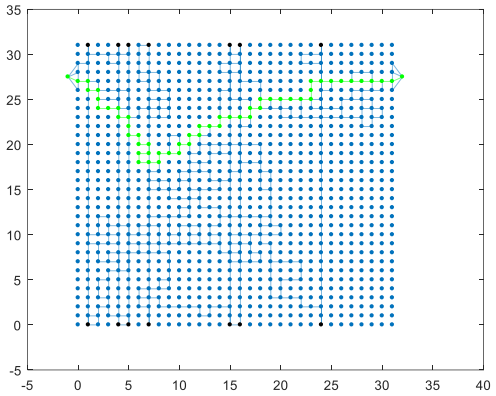

Figure 63: The shortest gas path in green, the gas backbone in

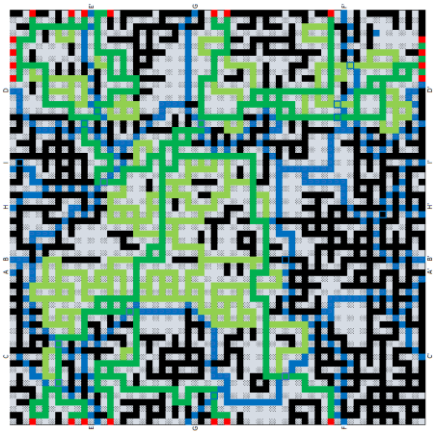

Figure 64: The water and gas paths.

Table 18: The total conductivity of the gas network is given by C gas in Hadjisotiriou. The resistance of the gas network is given by R gas. The tables show the counts for the flow geometries and the total resistance per flow path. To the right of the tables the total resistance for the horizontal and vertical directions are given for both the slip and no slip conditions.

C gas	R gas							
0.0562	17.79359							
Horizontal							All Horizontal paths	
	R1	R1	R2	Rb	R Slip	R No Slip	R slip	R no slip
AA'	47	41	5	3	445.34	565.75	74.35801	93.72911
BB'	55	51	3	2	475.20	593.08		
CC'	38	32	5	3	375.60	480.68		
DD'	56	52	1	2	452.48	555.79		
HH'	50	44	5	3	468.59	594.11		
II'	51	43	5	4	478.00	605.11		
Vertical							All Vertical paths	
	R1	R1	R2	Rb	R Slip	R No Slip	R slip	R no slip
EE'	43	37	9	3	475.28	621.43	142.4027	184.1548
FF'	35	27	7	4	384.49	500.62		
GG'	45	37	5	4	431.51	548.40		

Network 11 (p=0,46)

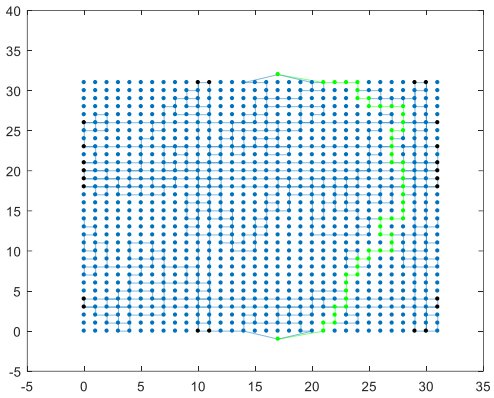

Figure 65: The shortest gas path in green, the gas backbone in

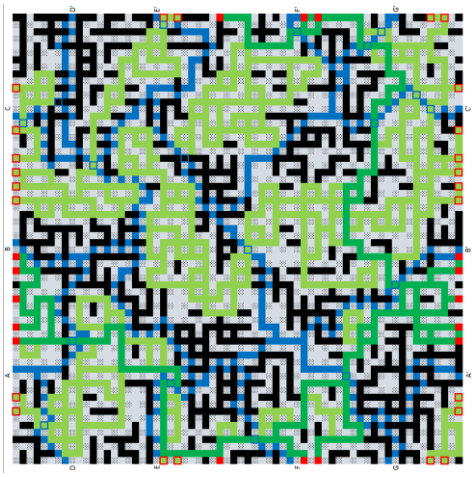

Figure 66: The water and gas paths.

Table 19: The total conductivity of the gas network is given by C gas in Hadjisotiriou. The resistance of the gas network is given by R gas. The tables show the counts for the flow geometries and the total resistance per flow path. To the right of the tables the total resistance for the horizontal and vertical directions are given for both the slip and no slip conditions.

C gas	R gas							
0.0661	15.12859							
Horizontal							All Horizontal paths	
	R1	R1	R2	Rb	R Slip	R No Slip	R slip	R no slip
AA'	55	51	11	2	597.06	780.05	187.5887	241.9187
BB'	54	50	8	2	543.61	700.49		
CC'	56	44	7	6	550.54	702.21		
Vertical							All Vertical paths	
	R1	R1	R2	Rb	R Slip	R No Slip	R slip	R no slip
DD'	51	43	6	4	493.23	628.48	107.3361	135.8962
EE'	49	45	11	2	550.57	723.34		
FF'	43	37	2	3	368.65	457.83		
GG'	40	32	3	4	362.30	454.39		

Network 12 (p=0,54)

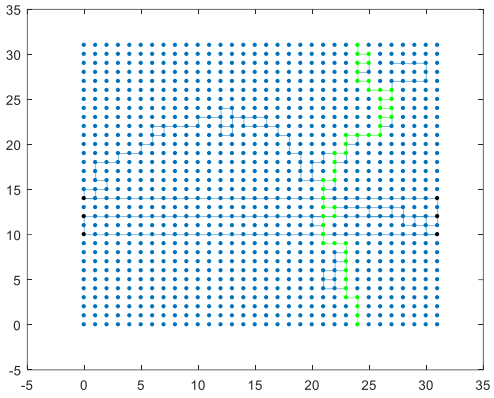

Figure 67: The shortest gas path in green, the gas backbone in

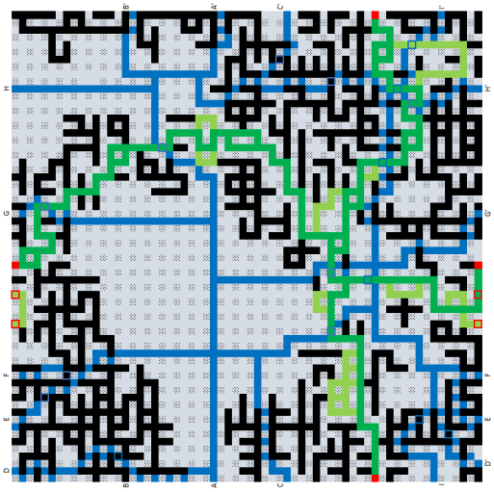

Figure 68: The water and gas paths.

Table 20: The total conductivity of the gas network is given by C gas in Hadjisotiriou. The resistance of the gas network is given by R gas. The tables show the counts for the flow geometries and the total resistance per flow path. To the right of the tables the total resistance for the horizontal and vertical directions are given for both the slip and no slip conditions.

C gas	R gas							
0.0244	40.98361							
Horizontal							All Horizontal paths	
	R1	R1	R2	Rb	R Slip	R No Slip	R slip	R no slip
DD'	28	22	4	3	282.88	362.79	38.0904	48.75359
EE'	21	17	2	2	196.51	248.33		
FF'	12	8	3	2	142.01	186.64		
GG'	18	14	1	2	158.04	196.61		
HH'	22	18	4	2	234.73	304.53		
Vertical							All Vertical paths	
	R1	R1	R2	Rb	R Slip	R No Slip	R slip	R no slip
AA'	7	5	1	1	71.14	91.08	31.29713	40.94861
BB'	7	5	4	1	116.84	161.20		
CC'	15	11	4	2	180.49	238.36		
II'	29	19	2	5	263.50	328.60		

B4. COMSOL models

Global definitions

To change the dimensions of the models easily, two global parameters must be set.

In the Model Builder window right click on Global Definitions and click Parameters. In Parameters 1 recreate the following table:

Name	Expression	Value
H	2	2
R	1	1

Basic shapes

It is possible to create Geometry parts as part of the Global Definitions which can later be combined to create more complex shapes.

Three separate Shapes must be created, repeat the following steps for every 3D Part object:

In the Model Builder window right click on Global Definitions and click Geometry Parts→3D Part.

This creates the first Part. In its settings tab the following changes are made:

1. The Input Parameters are:

Name	Default expressic	Value
height	H	2
r	R	1

2. Change the Length unit to: "µm"

Part 1

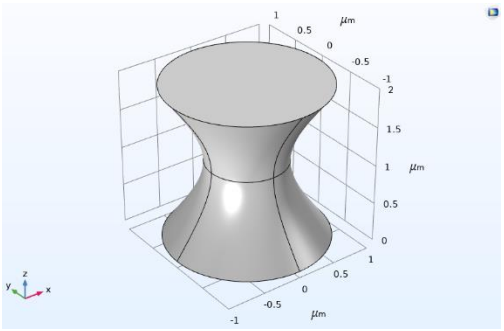

The following steps will create the first shape that represents a pillar with water around it.

1. Right-click Part 1 and click Work plane, this creates wp1.

2. Right-click Work Plane 1→Plane Geometry and click Circle, this creates c1.
   In the Settings of Circle 1 set the Radius to: "r".

3. Right-click Part 1 and click Work plane, this creates wp2.

4. In the Settings of Work Plane 2 set the z-coordinate to: "height/2".

5. Right-click Work Plane 2→Plane Geometry and click Circle, this creates c2.
   In the Settings of Circle 2 set the Radius to: "r/2".

6. Right-click Part 1 and click Transforms→Copy.
   In the Settings of Copy 1: Select wp1 as an Input Object.
   Enable Keep input objects.
   In Displacement set z: "height".

7. Right-click Part 1 and click Loft, this creates loft1.
   In the Settings of Loft 1 select the following as Profile Objects: wp1, wp2, and copy1.

Part 2

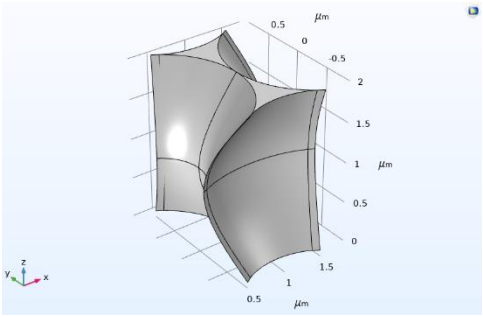

The following steps will create the second shape that represents the water-filled pore throat.

1. Right-click Part 2 and click Work plane, this creates wp1.

2. Right-click Work Plane 1→Plane Geometry and click Circle, this creates c1.
   In the Settings of Circle 1 set the Radius to "r".

3. Right-click Work Plane 1→Plane Geometry and click Circle, this creates c2.
   In the Settings of Circle 2 set the Radius to "r" and Position, xw to: "r*2".

4. Right-click Work Plane 1→Plane Geometry and click Booleans and Partitions→Union, this creates uni1.
   In the Settings of Union 1 select the following as Input Objects: c1, c2.

5. Right-click Work Plane 1→Plane Geometry and click Quadratic Bézier, this creates qb1.
   In the Settings of Quadratic Bézier 1 input the following values:

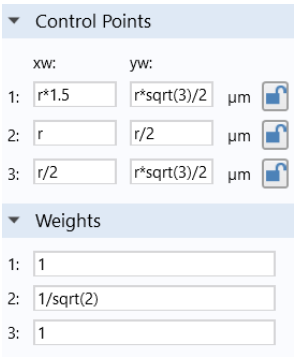

6. Right-click Work Plane 1→Plane Geometry and click Transforms→Mirror, this creates mir1.
   In the Settings of Mirror 1: Select qb1 as an Input Object.
   Set Normal Vector to Line of Reflection, xw to: "0".
   Set Normal Vector to Line of Reflection, xw to: "1".
7. Right-click Work Plane 1→Plane Geometry and click Conversions→Convert to Solid, this creates csol1.
   In the Settings of Convert to Solid 1, select the following as Input Objects: uni1, qb1, mir1.

8. Right-click Work Plane 1→Plane Geometry and click Booleans and Partitions→Union, this creates uni2.
   In the Settings of Union 2: Select the following as Input Objects: csol1.
   Select Repair tolerance: "Absolute".
   Set Absolute repair tolerance to: "3E-4".

9. Right-click Part 2 and click Copy, this creates copy1.
   In the Settings of Copy 1: Select wp1 as an Input Object.
   Enable Keep input objects.
   Set Displacement, z to: "height".

10. Right-click Part 2 and click Work plane, this creates wp2.
    In the Settings of Work Plane 2 set z-coordinate to: "height/2".

11. Right-click Work Plane 2→Plane Geometry and click Circle, this creates c1.
    In the Settings of Circle 1 set the Radius to "r".

12. Right-click Work Plane 2→Plane Geometry and click Circle, this creates c2.
    In the Settings of Circle 2 set the Radius to "r" and Position, xw to: "r*2".

13. Right-click Work Plane 2→Plane Geometry and click Booleans and Partitions→Union, this creates uni1.
    In the Settings of Union 1 select the following as Input Objects: c1, c2.

14. Right-click Work Plane 2→Plane Geometry and click Quadratic Bézier, this creates qb1.
    In the Settings of Quadratic Bézier 1 input the following values:

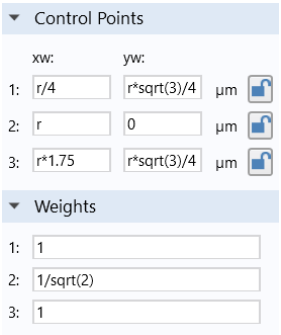

15. Right-click Work Plane 2→Plane Geometry and click Transforms→Mirror, this creates mir1.
    In the Settings of Mirror 1: Select qb1 as an Input Object.
    Set Normal Vector to Line of Reflection, xw to: "0".

Set Normal Vector to Line of Reflection, yw to: "1".

16. Right-click Work Plane 2→Plane Geometry and click Conversions→Convert to Solid, this creates csol1.
    In the Settings of Convert to Solid 1 select the following as Input Objects: uni1, qb1, mir1.

17. Right-click Work Plane 2→Plane Geometry and click Booleans and Partitions→Union, this creates uni2.
    In the Settings of Union 2 select the following as Input Objects: csol1.

18. Right-click Work Plane 2→Plane Geometry and click Booleans and Partitions→Partition Edges, this creates pare1.
    In the Settings of Partition Edges 1: Select edges 5 & 6 of uni2. (In the graphics window.)
    Set Relative arc length parameters to: "0.05"
    "0.95"

19. Right-click Part 2 and click Loft, this creates loft1.
    In the Settings of Loft 1: Enable Keep intermediate profile faces.
    Select as Profile Objects: wp1, wp2, and copy1.

20. Right-click Part 2 and click Parts→Part 1, this creates pi1.

21. Right-click Part 2 and click Parts→Part 1, this creates pi2.
    In the Settings of Part 1 2 (pi2) set Displacement, xw to: "r*2".

22. Right-click Part 2 and click Booleans and Partitions→Difference, this creates dif1.
    In the settings of Difference 1: Select as Objects to add: loft1.
    Select as Objects to subtract: pi1, pi2.
    Set Repair tolerance to: "Relative".
    Set Relative repair tolerance to: "1E-6".

Part 3

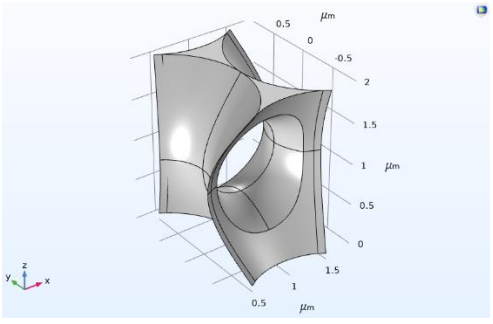

The following steps will create the third shape that represents the liquid bridge.

1. Right-click Part 3 and click Parts→Part 1, this creates pi1.

2. Right-click Part 3 and click Parts→Part 2, this creates pi2.
    In the settings of Part 1 (pi1): Change the Expression value for r to: "r*0.9".

Change the Expression value for height to: "r*1.5".

3. Right-click Part 3 and click Booleans and Partitions→Difference, this creates dif1.
   In the settings of Difference 1: Select as Object to add: pi2.
   Select as Object to subtract: pi1.

Flow Geometries

The three basic shapes are combined to form the basis for the eight different flow geometries. The flow geometries have separate COMSOL project files. They are created in the Model Builder window of COMSOL under Component 1→Geometry 1.

R1

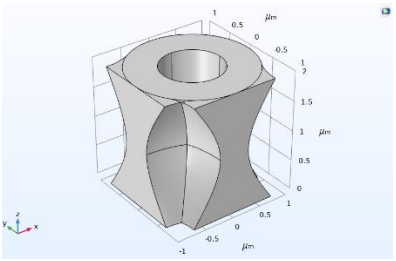

1. Right-click Geometry 1 and click Parts→Part 1, this creates pi1.

2. Right-click Geometry 1 and click Parts→Part 2, this creates pi2.
   In the settings of Part 2 1 (pi2) change the value for Rotation, Rotation angle to: "270".

3. Right-click Geometry 1 and click Parts→Part 2, this creates pi3.
   In the settings of Part 2 2 (pi3) change the value for Displacement, xw to: "-2*R".

4. Right-click Geometry 1 and click Selection→Box Selection, this creates boxsel1.
   In the settings of Box Selection 1 set the Geometric Entity Level to: "Object".

5. Right-click Geometry 1 and click Booleans and Partitions→Union, this creates uni1.
   In the settings of Union 1: Change Input objects to Box Selection 1.
   Uncheck Keep interior boundaries.

6. Right-click Geometry 1 and click Block, this creates blk1.
   In the settings of Block 1: Set Size and Shape, Width to: "R".
   Depth to: "2*R".
   Height to: "H".
   Set Position, x to: "-2*R".
   y to: "-R".

1. Right-click Geometry 1 and click Block, this creates blk2.
   In the settings of Block 2: Set Size and Shape, Width to: "2*R".
   Depth to: "R".
   Height to: "H".

	Set Position,	x to: "-R".
		y to: "-2*R".

2. Right-click Geometry 1 and click Cylinder, this creates cyl1.

In the settings of Cylinder 1:	Set Size and Shape,	Radius to: "R/2".
		Height to: "H".

3. Right-click Geometry 1 and click Booleans and Partitions→Difference, this creates dif1.

In the settings of Difference 1:	Select as Object to add: uni1.
	Select as Object to subtract: blk1, blk2, cyl1.

R2

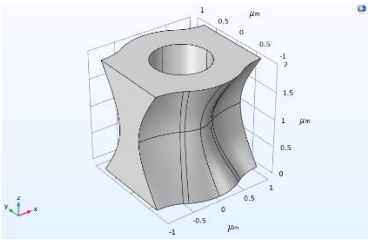

4. Right-click Geometry 1 and click Parts→Part 1, this creates pi1.

5. Right-click Geometry 1 and click Parts→Part 2, this creates pi2.

6. Right-click Geometry 1 and click Parts→Part 2, this creates pi3.

In the settings of Part 2 2 (pi3)	Set Displacement, xw to: "-2*R".

7. Right-click Geometry 1 and click Selection→Box Selection, this creates boxsel1.

In the settings of Box Selection 1	Set Geometric Entity Level to: "Object".

8. Right-click Geometry 1 and click Booleans and Partitions→Union, this creates uni1.

In the settings of Union 1:	Change Input objects to Box Selection 1.
	Uncheck Keep interior boundaries.

9. Right-click Geometry 1 and click Block, this creates blk1.

In the settings of Block 1:	Set Size and Shape,	Width to: "R".
		Depth to: "2*R".
		Height to: "H".
	Set Position,	x to: "-2*R".
		y to: "-R".

10. Right-click Geometry 1 and click Block, this creates blk2.

In the settings of Block 2:	Set Size and Shape,	Width to: "R".
		Depth to: "2*R".
		Height to: "H".
	Set Position,	x to: "R".
		y to: "-R".

11. Right-click Geometry 1 and click Cylinder, this creates cyl1.

In the settings of Cylinder 1: Set Size and Shape, Radius to: "R/2".
Height to: "H".

12. Right-click Geometry 1 and click Booleans and Partitions→Difference, this creates dif1.
In the settings of Difference 1: Select as Object to add: uni1.
Select as Object to subtract: blk1, blk2, cyl1.

Rb1

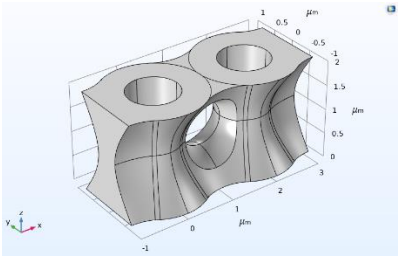

1. Right-click Geometry 1 and click Parts→Part 1, this creates pi1.

2. Right-click Geometry 1 and click Parts→Part 1, this creates pi2.
In the settings of Part 1 2 (pi2) Set Displacement, xw to: "2*R".

3. Right-click Geometry 1 and click Parts→Part 2, this creates pi3.
In the settings of Part 1 2 (pi3) Set Displacement, xw to: "-2*R".

4. Right-click Geometry 1 and click Parts→Part 2, this creates pi4.
In the settings of Part 1 2 (pi4) Set Displacement, xw to: "2*R".

5. Right-click Geometry 1 and click Parts→Part 3, this creates pi5.

6. Right-click Geometry 1 and click Selection→Box Selection, this creates boxsel1.
In the settings of Box Selection 1 Set Geometric Entity Level to: "Object".

7. Right-click Geometry 1 and click Booleans and Partitions→Union, this creates uni1.
In the settings of Union 1: Change Input objects to Box Selection 1.
Uncheck Keep interior boundaries.

8. Right-click Geometry 1 and click Block, this creates blk1.
In the settings of Block 1: Set Size and Shape, Width to: "R".
Depth to: "2*R".
Height to: "H".
Set Position, x to: "-2*R".
y to: "-R".

9. Right-click Geometry 1 and click Block, this creates blk2.
In the settings of Block 2: Set Size and Shape, Width to: "R".
Depth to: "2*R".
Height to: "H".

Set Position, x to: "3R".
y to: "-R".

10. Right-click Geometry 1 and click Cylinder, this creates cyl1.
    In the settings of Cylinder 1: Set Size and Shape, Radius to: "R/2".
    Height to: "H".

11. Right-click Geometry 1 and click Cylinder, this creates cyl2.
    In the settings of Cylinder 2: Set Size and Shape, Radius to: "R/2".
    Height to: "H".
    Set Position, x to: "2*R".

12. Right-click Geometry 1 and click Booleans and Partitions→Difference, this creates dif1.
    In the settings of Difference 1: Select as Object to add: uni1.
    Select as Object to subtract: blk1, blk2, cyl1, cyl2.

Rb2

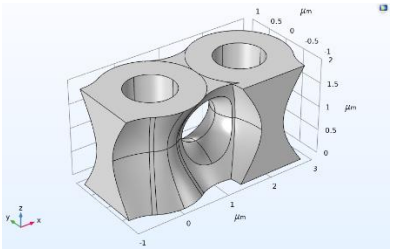

1. Right-click Geometry 1 and click Parts→Part 1, this creates pi1.
2. Right-click Geometry 1 and click Parts→Part 1, this creates pi2.
   In the settings of Part 1 2 (pi2) Set Displacement, xw to: "2*R".

3. Right-click Geometry 1 and click Parts→Part 2, this creates pi3.
   In the settings of Part 1 2 (pi3) Set Rotation, Rotation angle to "270".

4. Right-click Geometry 1 and click Parts→Part 2, this creates pi4.
   In the settings of Part 1 2 (pi4) Set Displacement, xw to: "2*R".
   Set Rotation, Rotation angle to "270".

5. Right-click Geometry 1 and click Parts→Part 3, this creates pi5.

6. Right-click Geometry 1 and click Selection→Box Selection, this creates boxsel1.
   In the settings of Box Selection 1 Set Geometric Entity Level to: "Object".

7. Right-click Geometry 1 and click Booleans and Partitions→Union, this creates uni1.
   In the settings of Union 1: Change Input objects to Box Selection 1.
   Uncheck Keep interior boundaries.

8. Right-click Geometry 1 and click Block, this creates blk1.

In the settings of Block 1:	Set Size and Shape,	Width to: "2*R". Depth to: "R". Height to: "H".
	Set Position,	x to: "-R". y to: "-2*R".

9. Right-click Geometry 1 and click Block, this creates blk2.

In the settings of Block 2:	Set Size and Shape,	Width to: "2*R". Depth to: "R". Height to: "H".
	Set Position,	x to: "R". y to: "-2*R".

10. Right-click Geometry 1 and click Cylinder, this creates cyl1.

In the settings of Cylinder 1:	Set Size and Shape,	Radius to: "R/2". Height to: "H".

11. Right-click Geometry 1 and click Cylinder, this creates cyl2.

In the settings of Cylinder 2:	Set Size and Shape,	Radius to: "R/2". Height to: "H".
	Set Position,	x to: "2*R".

12. Right-click Geometry 1 and click Booleans and Partitions→Difference, this creates dif1.

In the settings of Difference 1:	Select as Object to add: uni1. Select as Object to subtract: blk1, blk2, cyl1, cyl2.

Rb3

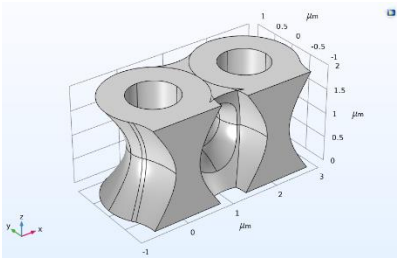

1. Right-click Geometry 1 and click Parts→Part 1, this creates pi1.

2. Right-click Geometry 1 and click Parts→Part 1, this creates pi2.

In the settings of Part 1 2 (pi2)	Set Displacement, xw to: "2*R".

3. Right-click Geometry 1 and click Parts→Part 2, this creates pi3.

In the settings of Part 1 2 (pi3)	Set Rotation, Rotation angle to "270".

4. Right-click Geometry 1 and click Parts→Part 2, this creates pi4.

In the settings of Part 1 2 (pi4)	Set Displacement, xw to: "2*R".	
	Set Rotation, Rotation angle to "270".	

5. Right-click Geometry 1 and click Parts→Part 3, this creates pi5.

6. Right-click Geometry 1 and click Selection→Box Selection, this creates boxsel1.

In the settings of Box Selection 1	Set Geometric Entity Level to: "Object".	

7. Right-click Geometry 1 and click Booleans and Partitions→Union, this creates uni1.

In the settings of Union 1:	Change Input objects to Box Selection 1.	
	Uncheck Keep interior boundaries.	

8. Right-click Geometry 1 and click Block, this creates blk1.

In the settings of Block 1:	Set Size and Shape,	Width to: "R".
		Depth to: "2*R".
		Height to: "H".
	Set Position,	x to: "-2*R".
		y to: "-R".

9. Right-click Geometry 1 and click Block, this creates blk2.

In the settings of Block 2:	Set Size and Shape,	Width to: "2*R".
		Depth to: "R".
		Height to: "H".
	Set Position,	x to: "R".
		y to: "-2*R".

10. Right-click Geometry 1 and click Cylinder, this creates cyl1.

In the settings of Cylinder 1:	Set Size and Shape,	Radius to: "R/2".
		Height to: "H".

11. Right-click Geometry 1 and click Cylinder, this creates cyl2.

In the settings of Cylinder 2:	Set Size and Shape,	Radius to: "R/2".
		Height to: "H".
	Set Position,	x to: "2*R".

12. Right-click Geometry 1 and click Booleans and Partitions→Difference, this creates dif1.

In the settings of Difference 1:	Select as Object to add: uni1.
	Select as Object to subtract: blk1, blk2, cyl1, cyl2.

Rb4

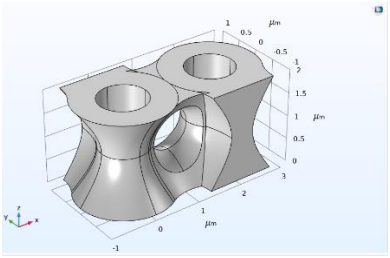

1. Right-click Geometry 1 and click Parts→Part 1, this creates pi1.

2. Right-click Geometry 1 and click Parts→Part 1, this creates pi2.
   In the settings of Part 1 2 (pi2) — Set Displacement, xw to: "2*R".

3. Right-click Geometry 1 and click Parts→Part 2, this creates pi3.
   In the settings of Part 1 2 (pi3) — Set Rotation, Rotation angle to "90".

4. Right-click Geometry 1 and click Parts→Part 2, this creates pi4.
   In the settings of Part 1 2 (pi4) — Set Displacement, xw to: "2*R".
   Set Rotation, Rotation angle to "270".

5. Right-click Geometry 1 and click Parts→Part 3, this creates pi5.

6. Right-click Geometry 1 and click Selection→Box Selection, this creates boxsel1.
   In the settings of Box Selection 1 — Set Geometric Entity Level to: "Object".

7. Right-click Geometry 1 and click Booleans and Partitions→Union, this creates uni1.
   In the settings of Union 1: — Change Input objects to Box Selection 1.
   Uncheck Keep interior boundaries.

8. Right-click Geometry 1 and click Block, this creates blk1.
   In the settings of Block 1: — Set Size and Shape, Width to: "2*R".
   Depth to: "R".
   Height to: "H".
   Set Position, x to: "-R".
   y to: "R".

9. Right-click Geometry 1 and click Block, this creates blk2.
   In the settings of Block 2: — Set Size and Shape, Width to: "2*R".
   Depth to: "R".
   Height to: "H".
   Set Position, x to: "R".
   y to: "-2*R".

10. Right-click Geometry 1 and click Cylinder, this creates cyl1.
    In the settings of Cylinder 1: — Set Size and Shape, Radius to: "R/2".
    Height to: "H".

11. Right-click Geometry 1 and click Cylinder, this creates cyl2.
    In the settings of Cylinder 2: Set Size and Shape, Radius to: "R/2". Height to: "H". Set Position, x to: "2*R".

12. Right-click Geometry 1 and click Booleans and Partitions→Difference, this creates dif1.
    In the settings of Difference 1: Select as Object to add: uni1. Select as Object to subtract: blk1, blk2, cyl1, cyl2.

Rg

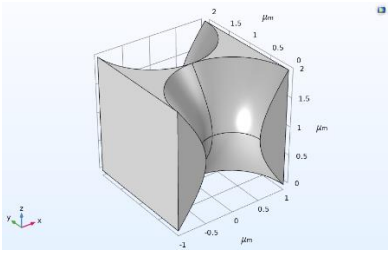

1. Right-click Geometry 1 and click Parts→Part 1, this creates pi1.

2. Right-click Geometry 1 and click Parts→Part 1, this creates pi2.
    In the settings of Part 1 2 (pi2) Set Displacement, yw to: "R*2".

3. Right-click Geometry 1 and click Parts→Part 2, this creates pi3.
    In the settings of Part 2 1 (pi3) Set Rotation, Rotation angle to: "90".

4. Right-click Geometry 1 and click Selection→Box Selection, this creates boxsel1.
    In the settings of Box Selection 1 Set Geometric Entity Level to: "Object".

5. Right-click Geometry 1 and click Booleans and Partitions→Union, this creates uni1.
    In the settings of Union 1: Change Input objects to Box Selection 1. Uncheck Keep interior boundaries.

6. Right-click Geometry 1 and click Block, this creates blk1.
    In the settings of Block 1: Set Size and Shape, Width to: "2*R". Depth to: "2*R". Height to: "H". Set Position, x to: "-R". y to: "R".

6. Right-click Geometry 1 and click Booleans and Partitions→Difference, this creates dif1.
    In the settings of Difference 1: Select as Object to add: blk1. Select as Object to subtract: uni1.

Rgb

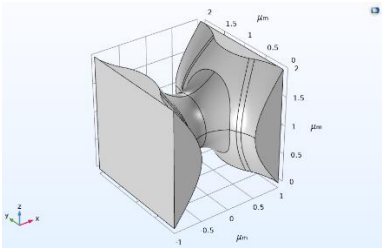

1. Right-click Geometry 1 and click Parts→Part 1, this creates pi1.

2. Right-click Geometry 1 and click Parts→Part 1, this creates pi2.
   In the settings of Part 1 2 (pi2) Set Displacement, yw to: "R*2".

3. Right-click Geometry 1 and click Parts→Part 3, this creates pi3.
   In the settings of Part 3 1 (pi3) Set Rotation, Rotation angle to "90".

4. Right-click Geometry 1 and click Selection→Box Selection, this creates boxsel1.
   In the settings of Box Selection 1 Set Geometric Entity Level to: "Object".

5. Right-click Geometry 1 and click Booleans and Partitions→Union, this creates uni1.
   In the settings of Union 1: Change Input objects to Box Selection 1.
   Uncheck Keep interior boundaries.

6. Right-click Geometry 1 and click Block, this creates blk1.
   In the settings of Block 1: Set Size and Shape, Width to: "2*R".
   Depth to: "2*R".
   Height to: "H".
   Set Position, x to: "-R".
   y to: "R".

6. Right-click Geometry 1 and click Booleans and Partitions→Difference, this creates dif1.
   In the settings of Difference 1: Select as Object to add: blk1.
   Select as Object to subtract: uni1.